Research Square

Preprints are preliminary reports that have not undergone peer review.
They should not be considered conclusive, used to inform clinical practice,
or referenced by the media as validated information.

Efficacy of Zongertinib in *ABCG2*-Dependent Trastuzumab Deruxtecan-Resistant HER2-Mutant Non-Small Cell Lung Cancer

Yusuke Kawanaka
Kindai University
Kimio Yonesaka
yonesaka@med.kindai.ac.jp
Kindai University
Kazuhiko Kuwahara
Kindai University
Waka Dohi
Kindai University
Takashi Kurosaki
Kindai University
Shinichiro Suzuki
Kindai University
Daiki Murata
Kindai University
Hiroaki Kanemura
Kindai University
Satomi Watanabe
Kindai University
Takayuki Takahama
Kindai University
Junko Tanizaki
Kindai University
Kaoru Tanaka
Kindai University
Toshiyuki Takehara
Kindai University
Takeshi Teramura
Kindai University
Kazuko Sakai

Kindai University
Yuta Yamanaka
Kansai Medical University
Yosuke Tamura
Osaka Medical and Pharmaceutical University
Shunsuke Misono
Kagoshima University
Eiji Iwama
Kyushu University
Kentaro Tanaka
Kyushu University
Yasuhito Fujisaka
Osaka Medical and Pharmaceutical University
Takayasu Kurata
Kansai Medical University
Isamu Okamoto
Kyushu University
Kazuto Nishio
Kindai University
Hidetoshi Hayashi
Kindai University

Article

Keywords: HER2, trastuzumab deruxtecan, zongertinib, ABCG2, NSCLC

Posted Date: November 10th, 2026

DOI: https://doi.org/10.21203/rs.3.rs-10782728/v1

License: This work is licensed under a Creative Commons Attribution 4.0 International License.
Read Full License

Additional Declarations: Competing interest reported. Y. Kawanaka reports receiving research funding from Nippon Boehringer Ingelheim Co., Ltd. K. Yonesaka reports receiving research funding from Nippon Boehringer Ingelheim Co., Ltd. and Boehringer Ingelheim International GmbH; grants from Daiichi Sankyo Co., Ltd.; honoraria from Daiichi Sankyo Co., Ltd., AstraZeneca K.K., Chugai Pharmaceutical Co., Ltd., Pfizer Japan Inc. and Amgen Inc.; patents planned and issued from Daiichi Sankyo Co., Ltd. T. Kurosaki reports receiving research funding from Nippon Boehringer Ingelheim Co., Ltd.; grants from Chugai Pharmaceutical Co., Ltd. S. Suzuki reports receiving research funding from Nippon Boehringer Ingelheim Co., Ltd.; grants from Boehringer Ingelheim Co., Ltd. H. Kanemura reports receiving grants from Chugai

Pharmaceutical Co., Ltd., Takeda Pharmaceutical Co., Ltd.; honoraria from Chugai Pharmaceutical Co., Ltd., AstraZeneca K.K., Daiichi Sankyo Co., Ltd., MSD K.K. and Novartis Pharma K.K. S. Watanabe reports receiving honoraria from Daiichi Sankyo Co., Ltd., Chugai Pharmaceutical Co., Ltd., MSD K.K., Eli Lilly Japan K.K., Kyowa Kirin Co., Ltd., and Eisai Co., Ltd., and Pfizer K.K., and serving on an advisory board for Daiichi Sankyo Co., Ltd. T. Takahama reports receiving honoraria from Chugai Pharmaceutical Co., Ltd. and AstraZeneca K.K. J. Tanizaki reports receiving honoraria from AstraZeneca K.K., AbbVie GK., Amgen Inc., Boehringer Ingelheim Japan Inc., Bristol-Myers Squibb Co. Ltd., Chugai Pharmaceutical Co., Ltd., Daiichi Sankyo Co., Ltd., Eli Lilly Japan K.K., Janssen Pharmaceutical K.K., Johnson & Johnson, MSD K.K., Ono Pharmaceutical Co., Ltd., Pfizer Japan Inc., Taiho Pharmaceutical Co. Ltd. and Takeda Pharmaceuticals, and serving on an advisory board for AstraZeneca K.K., Chugai Pharmaceutical Co., Ltd., Janssen Pharmaceutical K.K. and Pfizer Japan Inc. Kaoru Tanaka reports receiving honoraria from AstraZeneca K.K., Merck Biopharma Co., Ltd., Eisai Co., Ltd., Bristol-Myers Squibb K.K., Ono Pharmaceutical Co., Ltd., MSD K.K., Chugai Pharmaceutical Co., Ltd., Takeda Pharmaceutical Co., Ltd., Taiho Pharmaceutical Co., Ltd., Kyowa Kirin Co., Ltd. and Novartis Pharma K.K. K. Sakai reports receiving honoraria from Qiagen, Inc., Takeda Pharmaceutical Co., Ltd., Nippon Kayaku Co., Ltd., and Life Technologies Japan Ltd. Y. Tamura reports receiving honoraria from MSD K.K., Chugai Pharmaceutical Co., Ltd., AstraZeneca K.K., Ono Pharmaceutical Co., Ltd., and Boehringer Ingelheim Japan Inc.; grants from AbbVie Inc., Ono Pharmaceutical Co. Ltd., and Shanghai Junshi Biosciences Co., Ltd. E. Iwama reports personal fees from AstraZeneca and Chugai Pharmaceutical. Kentaro Tanaka reports serving on the advisory council with AstraZeneca and Pfizer; speaker's bureau with AstraZeneca, Bristol Myers Squibb, Chugai Pharmaceutical, Merck, Merck Sharp & Dohme, and Ono Pharmaceutical. Y. Fujisaka reports receiving honoraria from Eli Lilly Japan K.K., AstraZeneca, Chugai Pharmaceutical Co., Ltd., Pfizer Japan Inc., Ono Pharmaceutical Co., Ltd., Daiichi Sankyo Co., Ltd, and Taiho Pharmaceutical Co. Ltd.; grants from Summit Therapeutics Sub, Taiho Pharmaceutical Co., Ltd., MSD K.K., Daiichi Sankyo Co., Ltd., Bristol-Myers Squibb Co., Ltd., Genmab K.K., Pfizer Japan Inc., Kyowa Kirin Co., Ltd., AbbVie GK, and Ono Pharmaceutical Co., Ltd. T. Kurata reports personal fees from MSD, Ono Pharmaceutical, Bristol-Myers Squibb, AstraZeneca, Chugai Pharma, and Janssen Pharmaceuticals, and grants from MSD, Daiichi Sankyo, Chugai Pharma, Amgen, Janssen Pharmaceuticals, BeOne, SUMMIT, and Regeneron. I. Okamoto reports receiving grants from Chugai Pharmaceutical, AstraZeneca, Taiho Pharmaceutical, Boehringer Ingelheim, Ono Pharmaceutical, MSD, Eli Lilly, Astellas, Bristol Myers Squibb, Novartis, Pfizer, and AbbVie; consulting fees from AstraZeneca, Bristol Myers Squibb, and AbbVie; and personal fees from AstraZeneca, Taiho Pharmaceutical, Boehringer Ingelheim, Chugai Pharmaceutical, Ono Pharmaceutical, MSD, Eli Lilly, Bristol-Myers Squibb, Novartis, and Pfizer. K. Nishio reports receiving grants from West Japan Oncology Group, Hitachi Ltd., Otsuka Pharmaceutical Co., Ltd., Thoracic Oncology Research Group, Eli Lilly Japan K.K., Okayama University, Japan Breast Cancer Research Group, Nippon Boehringer Ingelheim Co., Ltd., and Kyushu Study Group of Clinical Cancer; consulting fees from SymBio Pharmaceuticals Ltd., Eli Lilly Japan K.K., and Otsuka Pharmaceutical Co., Ltd.; and honoraria from Chugai Pharmaceutical Co., Ltd., MSD K.K., Guardant Health, Janssen Pharmaceutical K.K., Eli Lilly Japan K.K., AstraZeneca K.K., Nichirei Biosciences Inc., and Maruho Co., Ltd. H. Hayashi reports grants from IQVIA Services JAPAN K.K., SYNEOS HEALTH CLINICAL K.K., EPS Corporation.,

Nippon Kayaku Co., Ltd., Takeda Pharmaceutical Co., Ltd., MSD K.K., Amgen Inc., Taiho Pharmaceutical Co., Ltd., Bristol Myers Squibb Company, Janssen Pharmaceutical K.K., CMIC CO., Ltd., Pfizer R&D Japan G.K., Labcorp Development Japan K.K., Kobayashi Pharmaceutical Co., Ltd., Pfizer Japan Inc., AbbVie Inc., A2 Healthcare Corp., Eisai Co., Ltd., EP-CRSU CO., LTD., Shionogi & Co., Ltd., Otsuka Pharmaceutical Co., Ltd., GlaxoSmithKline K.K., Sanofi K.K., Chugai Pharmaceutical Co., Ltd., Nippon Boehringer Ingelheim Co., Ltd., SRL Medisearch Inc., PRA Health Sciences Inc., Astellas Pharma Inc., Ascent Development Services, Eisai Inc., Bayer Yakuhin, Ltd., AstraZeneca K.K., Daiichi Sankyo Co., Ltd., Novartis Pharma K.K., Eli Lilly Japan K.K., Medpace Japan K.K., Japanese Gastric Cancer Association, Clinical Research Support Center Kyushu, Japan Clinical Cancer Research Organization, Merck Biopharma Co., Ltd, Kyowa Kirin Co., Ltd., Thoracic Oncology Research Group, West Japan Oncology Group, Comprehensive Support Project for Oncological Research of Breast Cancer, Mochida Pharmaceutical Co., Ltd., MSD K.K., Sysmex Corporation., Public Health Research Foundation., ICON Japan K.K. and PPD-SNBL K.K.; honoraria from Ono Pharmaceutical Co., Ltd., Daiichi Sankyo Co., Ltd., AstraZeneca K.K., Chugai Pharmaceutical Co., Ltd., Eli Lilly Japan K.K., MSD K.K., Pfizer Japan Inc., Nippon Boehringer Ingelheim Co., Ltd., Guardant Health Japan Corp., Merck Biopharma Co., Ltd., 3H Clinical Trial Inc., Novartis Pharma K.K., Bristol Myers Squibb Company, Amgen Inc., Sysmex Corporation, Takeda Pharmaceutical Co., Ltd. and Janssen Pharmaceutical K.K., AbbVie Inc., Kyowa Kirin Co., Ltd., Reno. Medical K.K., Nippon Kayaku Co., Ltd., Hisamitsu Pharmaceutical Co., Inc., Novocure K.K., Eisai Co., Ltd., Care Net, Inc., Taiho Pharmaceutical Co., Ltd., 3H Clinical Trial Inc., Ishiyaku Publishers, Inc. and Medical Review Co., Ltd.; participation in a data safety monitoring board or advisory board for Bristol Myers Squibb Company, Chugai Pharmaceutical Co., Ltd., AstraZeneca K.K., Janssen Pharmaceutical K.K., AbbVie Inc., Novocure K.K., and Daiichi Sankyo Co., Ltd. The other authors declare no competing interests.

Abstract

Resistance to trastuzumab deruxtecan (T-DXd) limits treatment options for HER2-mutant non-small cell lung cancer (NSCLC). We investigated resistance mechanisms and zongertinib activity using T-DXd-resistant cells, patient tumor specimens, and patient-derived organoids (PDOs). Comparative analyses identified upregulation of ATP-binding cassette transporter G2 (ABCG2) in resistant cells. ABCG2 expression increased after T-DXd treatment in five of six paired tumor specimens. ABCG2 knockdown enhanced T-DXd sensitivity in resistant cells, while pharmacological inhibition enhanced sensitivity in resistant PDOs. HER2 signaling remained active in resistant models, and zongertinib inhibited HER2 phosphorylation and organoid growth. Tumor shrinkage was also observed in the corresponding patients treated with zongertinib. These findings provide patient-linked evidence implicating ABCG2 in acquired T-DXd resistance and suggest that HER2 signaling remains therapeutically targetable with zongertinib after T-DXd resistance in HER2-mutant NSCLC.

Introduction

Human epidermal growth factor receptor 2 (HER2) belongs to the epidermal growth factor receptor (EGFR) family, along with HER1, HER3, and HER4. Activating HER2 tyrosine kinase mutations or HER2 overexpression cause autophosphorylation or transphosphorylation of cytoplasmic tyrosine residues in HER2 and other HER family members, activating multiple intracellular signaling pathways (1, 2). In non-small cell lung cancer (NSCLC), *HER2* mutations, particularly exon 20 insertions, account for approximately 2–4% of cases and represent a distinct oncogenic driver (3–5). Accordingly, *HER2* mutations have recently emerged as important therapeutic targets.

Trastuzumab deruxtecan (T-DXd) is a HER2-targeted antibody—drug conjugate (ADC) comprising an anti-HER2 monoclonal antibody, a cleavable peptide linker, and a topoisomerase I inhibitor payload called deruxtecan (DXd) (6, 7). T-DXd therapy has emerged as a standard treatment for multiple malignancies (8–11). In HER2-mutant NSCLC, T-DXd achieved objective response rates > 50% and a median progression-free survival (PFS) of approximately 8–9 months in two phase II trials, DESTINY-Lung01 and DESTINY-Lung02 (10, 12). Despite its potent antitumor effects, most patients eventually develop resistance, and the mechanisms underlying acquired resistance to T-DXd remain poorly understood. Although reduced HER2 expression is a major resistance mechanism in breast cancer, HER2-mutant NSCLC tumors inherently express lower HER2 levels than breast cancer cells (13–16). Therefore, clarifying these mechanisms is critical for improving therapeutic outcomes and developing postresistance treatment strategies.

Zongertinib, a novel selective HER2 tyrosine kinase inhibitor (TKI), has shown clinical activity in HER2-mutant NSCLC, including tumors harboring exon 20 insertions. The Beamion LUNG-1 trial evaluated its safety and efficacy in patients with HER2-mutant NSCLC (17), reporting a confirmed objective response rate of 71% and a median PFS of 12.4 months (17). Furthermore, subgroup analyses demonstrated high efficacy regardless of clinical characteristics, including sex, age, race, and smoking history (17). Unlike T-

DXd, which delivers a cytotoxic payload through HER2-mediated internalization, zongertinib directly inhibits HER2 kinase activity. Previous preclinical studies have suggested that HER2-targeted TKIs may retain antitumor activity after the acquisition of T-DXd resistance (18, 19). Nevertheless, clinical and patient-derived experimental evidence supporting the efficacy of zongertinib following T-DXd resistance remains limited, and the molecular determinants of differential susceptibility to these agents require further investigation.

With the emergence of T-DXd and zongertinib as therapeutic options for HER2-mutant NSCLC, understanding resistance mechanisms and identifying effective treatment strategies after disease progression have become increasingly important (20). In particular, integrating molecular analyses of resistant tumors with functional studies using patient-derived models may provide insights into the biological mechanisms underlying differential drug susceptibility. In this study, we investigated the molecular mechanisms of acquired T-DXd resistance using HER2-mutant NSCLC cell lines, tumor specimens, and patient-derived organoids (PDOs). We further evaluated the contribution of ATP-binding cassette transporter G2 (ABCG2) to T-DXd resistance and examined the antitumor activity of zongertinib in T-DXd-resistant HER2-mutant NSCLC models, with the aim of providing a biological rationale for subsequent treatment strategies.

Results

T-DXd-resistant cells exhibit reduced sensitivity to DXd despite preserved trafficking to acidic intracellular compartments

To explore the potential mechanisms of T-DXd resistance, we established resistant clones, including H1781DSR3 cells, by exposing these cells to increasing concentrations of T-DXd. A high-density cell growth assay demonstrated that 1 μg/mL T-DXd markedly inhibited cell growth in parental H1781 cells but not in H1781DSR3 cells (Fig. 1A). To assess T-DXd-induced apoptosis, we performed western blotting for cleaved poly(ADP-ribose) polymerase (PARP) and cleaved caspase 3 using H1781 and H1781DSR3 cells exposed to 1 μg/mL T-DXd for 72 h. T-DXd induced the expression of these proteins in parental H1781 cells but not in H1781DSR3 cells (Fig. 1B). We then evaluated HER2, the target of T-DXd, and its downstream ERK signaling pathway in these cells using western blotting. Total HER2 expression in the whole cell lysate of H1781DSR3 cells was comparable to that in the parental cells (Fig. 1C). HER2 phosphorylation was maintained in H1781DSR3 cells, indicating that HER2 signaling remained active despite acquired resistance to T-DXd (Fig. 1C). In addition, ERK phosphorylation was minimally reduced in both cell lines exposed to 1 μg/mL T-DXd (Fig. 1C). To evaluate T-DXd-induced DNA damage, we assessed phosphorylation of histone H2AX, a marker of DNA double-strand breaks. T-DXd exposure significantly increased the ratio of phosphorylated histone H2AX to total histone H2AX in parental H1781 cells compared with no exposure controls (Fig. 1D, E; $p = 0.0327$). In contrast, phosphorylated histone H2AX was not detectable in H1781DSR3 cells under the experimental conditions, despite detectable

total histone H2AX expression (Fig. 1D). These findings suggest that attenuated T-DXd-induced DNA damage is associated with the resistant phenotype.

Because reduced cell-surface HER2 expression could potentially limit T-DXd binding and internalization, we quantified cell-surface HER2 expression. Cell-surface HER2 expression was modestly but significantly lower in H1781DSR3 cells than in parental H1781 cells (Fig. 1F). To investigate whether T-DXd resistance was associated with impaired intracellular trafficking, we assessed the delivery of pHrodo-labeled T-DXd to acidic intracellular compartments by measuring fluorescence intensity. Despite reduced cell-surface HER2 expression, H1781DSR3 cells exhibited higher pHrodo fluorescence intensity than parental H1781 cells (Fig. 1G), suggesting that the delivery of T-DXd to acidic intracellular compartments, such as lysosomes, was not impaired in resistant cells. We next evaluated cellular sensitivity to DXd, the cytotoxic payload of T-DXd. H1781DSR3 cells exhibited a higher half-maximal inhibitory concentration (IC50) for DXd than parental H1781 cells (Fig. 1H, Supplementary Data), indicating reduced sensitivity to the payload itself. Collectively, these findings suggest that T-DXd resistance in H1781DSR3 cells is unlikely to be primarily attributable to impaired intracellular trafficking to acidic compartments, but may instead involve downstream mechanisms, including altered intracellular payload disposition or reduced sensitivity to DXd. Furthermore, targeted next-generation sequencing did not identify additional HER2 (ERBB2) mutations in H1781DSR3 cells compared with parental H1781 cells (Supplementary Fig. S1).

ABCG2 contributes to T-DXd resistance in HER2-mutant NSCLC

To further investigate the molecular basis of T-DXd resistance in H1781 cells, we performed transcriptomic profiling and pathway analysis of parental H1781 and T-DXd-resistant H1781DSR3 cells. Pathway analysis predicted significant enrichment of NRF2-related signaling in H1781DSR3 cells (Fig. 2A). NRF2 is a transcription factor involved in cancer progression, metastasis, and therapeutic resistance (21). NRF2 regulates the expression of several genes involved in drug metabolism and transport, including members of the aldo-keto reductase (AKR) superfamily and ATP-binding cassette (ABC) transporters (22, 23). Consistent with these findings, differential gene expression analysis revealed increased expression of AKR1C family members (*AKR1C1*, *AKR1C2*, and *AKR1C3*) and multiple ABC transporters, including *ABCG2*, which encodes breast cancer resistance protein (BCRP), in H1781DSR3 cells compared with parental H1781 cells (Fig. 2B, Supplementary Fig. S2). Increased protein expression of AKR1C and ABCG2 was further confirmed by western blotting (Fig. 2C).

Because DXd, the cytotoxic payload of T-DXd, has been reported to be a substrate of ABCG2-mediated drug efflux (24–26), we hypothesized that increased ABCG2 expression contributes to T-DXd resistance in H1781DSR3 cells. To investigate this possibility, we first evaluated the effects of febuxostat, an inhibitor of ABCG2-mediated transport, on T-DXd sensitivity using high-density growth assays. Parental H1781 cells were highly sensitive to 1 μg/mL T-DXd, whereas H1781DSR3 cells exhibited resistance to T-DXd (Fig. 2D). Treatment with 10 μM febuxostat alone had little effect on cell growth in either cell line. However, combined treatment with T-DXd and febuxostat markedly suppressed cell growth in

H1781DSR3 cells and further enhanced the growth-inhibitory effect of T-DXd in parental H1781 cells (Fig. 2D).

Because potential off-target effects of febuxostat could not be excluded, we further investigated the functional contribution of ABCG2 using genetic approaches. We first knocked down *ABCG2* expression in H1781DSR3 cells using siRNA (Fig. 2E). *ABCG2* knockdown significantly enhanced the growth-inhibitory effect of T-DXd compared with control siRNA transfection (Fig. 2F). Conversely, to determine whether increased ABCG2 expression was sufficient to confer T-DXd resistance, we ectopically expressed *ABCG2* in H1781 and H2170 cells, another NSCLC cell line (Fig. 2G). Although parental H1781 and H2170 cells were sensitive to 1 μg/mL T-DXd, their ABCG2-overexpressing counterparts, H1781ABCG2 and H2170ABCG2, exhibited reduced sensitivity to T-DXd (Fig. 2H). Together, these genetic loss- and gain-of-function experiments support a functional contribution of ABCG2 to T-DXd resistance in NSCLC cells.

To further evaluate the contribution of ABCG2 to sensitivity to DXd, the cytotoxic payload of T-DXd, we evaluated the effects of *ABCG2* knockdown on DXd sensitivity in H1781DSR3 cells. Dose–response analysis demonstrated that *ABCG2* knockdown reduced the IC50 of DXd from 8.594 nM in control siRNA-transfected cells to 4.081 nM in ABCG2 siRNA-transfected cells, indicating that ABCG2 contributes to DXd resistance in H1781DSR3 cells (Fig. 2I, Supplementary Data), corresponding to an approximately 2.1-fold increase in DXd sensitivity. These findings suggest that ABCG2 contributes to resistance to the cytotoxic payload of T-DXd. We also examined topoisomerase I (TOP1), the molecular target of DXd, and found no detectable differences in its expression or mutational status between parental H1781 and H1781DSR3 cells (Fig. 2B, Supplementary Fig. S1). Collectively, these findings support a functional role for ABCG2 in T-DXd resistance, potentially through reduced intracellular exposure to DXd.

We next investigated whether the resistant phenotype was maintained in vivo using xenograft models established from parental H1781 and H1781DSR3 cells. Immunohistochemical analysis demonstrated higher BCRP expression in H1781DSR3-derived tumors than in parental H1781-derived tumors (Fig. 2J). T-DXd treatment induced tumor regression in parental H1781 xenografts (Fig. 2K, Supplementary Data), whereas H1781DSR3 xenografts exhibited reduced responsiveness to T-DXd treatment (Fig. 2L, Supplementary Data). These findings indicate that the T-DXd-resistant phenotype of H1781DSR3 cells is maintained in vivo and is accompanied by increased BCRP expression, further supporting the potential involvement of ABCG2 in T-DXd resistance in HER2-mutant NSCLC.

Association between ABCG2 expression and resistance to T-DXd treatment in HER2-mutant NSCLC

Next, to investigate the clinical relevance of ABCG2 expression in HER2-mutant NSCLC, we performed immunohistochemical (IHC) analysis of BCRP, the protein encoded by *ABCG2*, using tumor specimens obtained before T-DXd treatment and after the development of resistance. Patient characteristics and BCRP expression scores are summarized in Fig. 3A. BCRP expression was evaluated based on membranous staining intensity and classified into four categories: 0, 1+, 2+, and 3+ (Fig. 3B). The

distribution of BCRP staining scores across all specimens is shown in Supplementary Fig. S3. For exploratory analyses, tumors were further categorized into low (0 or 1+) and high (2 + or 3+) BCRP expression groups.

We first examined the association between pretreatment BCRP expression and clinical outcomes following T-DXd therapy in 21 patients with HER2-mutant NSCLC. The clinical characteristics, treatment outcomes, and tumor specimen information of these patients are summarized in Supplementary Fig. S4. The distribution of BCRP expression scores in pretreatment tumor specimens from patients who received T-DXd is shown in Fig. 3C. The overall response rate was significantly higher in the low BCRP expression group (85.7%, 12/14 patients) than in the high BCRP expression group (0%, 0/7 patients; two-sided Fisher's exact test, $p < 0.05$; Fig. 3D). Patients with high pretreatment BCRP expression also showed a trend toward shorter progression-free survival (PFS) than those with low BCRP expression, although the association was not statistically significant (hazard ratio, 2.58; 95% confidence interval, 0.92–7.22; Fig. 3E).

We next investigated changes in BCRP expression following the development of acquired resistance to T-DXd. Paired tumor specimens obtained before T-DXd treatment and after disease progression were available from six patients. IHC images of these paired specimens are shown in Fig. 3F. BCRP expression increased after the development of resistance in five of the six patients, whereas it remained unchanged in one patient. However, the difference in BCRP expression scores between the paired pretreatment and post-progression specimens did not reach statistical significance (Wilcoxon matched-pairs signed-rank test, $p = 0.0625$; Fig. 3G).

Collectively, these findings suggest that elevated BCRP expression may be associated with reduced responsiveness to T-DXd and may contribute to acquired resistance in HER2-mutant NSCLC. However, given the limited sample size and exploratory nature of these analyses, further validation in larger independent cohorts is warranted.

ABCG2 inhibition restores sensitivity to T-DXd in T-DXd-resistant HER2-mutant NSCLC organoids

To further investigate the contribution of ABCG2 to T-DXd resistance in HER2-mutant NSCLC, we examined patient-derived organoids established from tumors with acquired resistance to T-DXd. Organoids were successfully established from cases #3 and #5, both of which exhibited high BCRP expression (IHC score 3+) in tumor specimens obtained after T-DXd resistance had developed (Figs. 3A and 4A). The clinical treatment courses, timing of tumor specimen collection, and PDO establishment for these patients are shown in Supplementary Fig. S5. Organoids derived from both cases exhibited progressive growth under untreated conditions (Fig. 4B–E). T-DXd treatment alone showed limited growth-inhibitory activity in both organoid models. In contrast, combined treatment with T-DXd and the ABCG2 inhibitor febuxostat markedly suppressed the growth of organoids derived from case #3 (Fig. 4B, C; Supplementary Data). Similarly, combined treatment with T-DXd and another ABCG2 inhibitor, Ko143,

suppressed the growth of organoids derived from case #5 (Fig. 4D, E, Supplementary Data). Neither ABCG2 inhibitor alone substantially affected organoid growth. These experiments involved longitudinal measurements of individual organoids cultured within the same well and were therefore interpreted descriptively.

To further validate these findings using independent experimental units, we performed an additional experiment with organoids derived from case #5. A single organoid was cultured in each independent well (n = 6 wells per treatment group) and exposed to T-DXd, febuxostat, or their combination. Relative organoid growth was calculated for each organoid based on the change in size from day 1 to day 13. Combined treatment with T-DXd and febuxostat significantly suppressed relative organoid growth compared with both the untreated control and T-DXd alone (Fig. 4F; Supplementary Data).

Together, these findings indicate that patient-derived organoids established from tumors with acquired resistance to T-DXd exhibit reduced sensitivity to T-DXd. The enhanced growth inhibition observed following combination treatment with T-DXd and two different ABCG2 inhibitors, together with elevated BCRP expression in the corresponding resistant tumors, supports a potential functional contribution of ABCG2 to acquired T-DXd resistance in HER2-mutant NSCLC.

Zongertinib retains antitumor activity in T-DXd-resistant HER2-mutant NSCLC by inhibiting HER2 signaling

Given its distinct mechanism of action from T-DXd, we investigated whether the HER2-selective tyrosine kinase inhibitor zongertinib retained antitumor activity in T-DXd-resistant HER2-mutant NSCLC. High-density growth assays demonstrated that H1781DSR3 cells remained sensitive to 100 nM zongertinib, with growth inhibition comparable to that observed in parental H1781 cells (Fig. 5A). Consistently, western blot analysis revealed increased levels of cleaved PARP and cleaved caspase 3 following zongertinib treatment in both H1781 and H1781DSR3 cells, indicating induction of apoptosis (Fig. 5B).

Because HER2 phosphorylation was maintained in H1781DSR3 cells despite acquired resistance to T-DXd (Fig. 1C), we next examined whether zongertinib inhibited HER2-mediated downstream signaling. Western blot analysis demonstrated that zongertinib suppressed the phosphorylation of HER2 and its downstream signaling molecules, AKT and ERK, in H1781DSR3 cells, with effects comparable to those observed in parental H1781 cells (Fig. 5C). These findings suggest that HER2 signaling remains active and pharmacologically targetable following the acquisition of T-DXd resistance.

To further investigate whether ABCG2 overexpression affected zongertinib sensitivity, we evaluated its antitumor activity in parental H1781 cells and ABCG2-overexpressing H1781ABCG2 cells. Although ABCG2 overexpression conferred resistance to T-DXd (Fig. 2H), treatment with 100 nM zongertinib inhibited cell growth in both cell lines, with no significant difference in the extent of reduction in cell viability between them (P = 0.37; Fig. 5D). These findings suggest that ABCG2 overexpression does not necessarily confer cross-resistance to zongertinib.

We next evaluated the in vivo antitumor activity of zongertinib using xenograft models established from H1781 and H1781DSR3 cells. In H1781-derived tumors, both T-DXd and zongertinib significantly inhibited tumor growth compared with the control group (Fig. 5E; Supplementary Data). In contrast, H1781DSR3-derived tumors exhibited reduced responsiveness to T-DXd, whereas zongertinib significantly inhibited tumor growth compared with both the control and T-DXd-treated groups at the final measurement (Fig. 5F; Supplementary Data). No significant differences in body weight were observed between the treatment and control groups (Supplementary Fig. S6).

Collectively, these findings demonstrate that zongertinib retains antitumor activity in T-DXd-resistant HER2-mutant NSCLC models, including those with increased ABCG2 expression. The suppression of HER2 downstream signaling and induction of apoptosis suggest that HER2 signaling remains therapeutically targetable despite acquired resistance to T-DXd (Supplementary Fig. S7). These findings support further investigation of zongertinib as a potential therapeutic option for HER2-mutant NSCLC following the development of T-DXd resistance.

Zongertinib exhibits antitumor activity in patient-derived models and patients with T-DXd-resistant HER2-mutant NSCLC

Finally, we investigated the antitumor activity of zongertinib using two patient-derived organoid (PDO) models established from patients with HER2-mutant NSCLC who had developed resistance to T-DXd (Patients 3 and 5). The clinical treatment courses of these patients are shown in Supplementary Fig. S5. Both PDO models exhibited detectable HER2 phosphorylation, which was markedly reduced to 10% or less of the untreated control levels following zongertinib treatment (Fig. 6A, B).

We next evaluated the effects of T-DXd and zongertinib on organoid growth. Longitudinal monitoring demonstrated that T-DXd had little effect on organoid growth, whereas zongertinib markedly suppressed growth in both PDO models (Fig. 6C, D for Patient 3; Fig. 6F, G for Patient 5). Because multiple organoids within each treatment group were cultured in a single well, these experiments were considered descriptive and were not subjected to statistical comparisons. The underlying raw data are provided in Supplementary Data.

To further assess the reproducibility of these findings, we conducted an independent experiment using PDOs derived from patient 5, in which individual organoids were cultured in separate wells (six independent wells per treatment group, with one organoid per well). After 13 days of treatment, zongertinib significantly suppressed organoid growth compared with both the vehicle control and T-DXd groups (both $P < 0.0001$), whereas T-DXd did not significantly affect growth compared with the vehicle control (Fig. 6I; Supplementary Data).

We also examined the clinical courses of patients 3 and 5, both of whom received zongertinib at a dose of 120 mg orally once daily after developing resistance to T-DXd. Their treatment histories and clinical

courses are presented in Supplementary Fig. S5. Computed tomography revealed reductions in the sizes of the illustrated tumor lesions during zongertinib treatment in both patients (Fig. 6E, H).

Collectively, these findings indicate that zongertinib retains antitumor activity in HER2-mutant NSCLC models with acquired resistance to T-DXd and suggest that HER2 signaling may remain therapeutically targetable after T-DXd resistance develops.

Discussion

In this study, increased ABCG2 expression was observed in HER2-mutant NSCLC with acquired resistance to T-DXd. Pharmacological inhibition and siRNA-mediated knockdown of ABCG2 restored sensitivity to T-DXd, suggesting that ABCG2 upregulation contributes to acquired T-DXd resistance in HER2-mutant NSCLC. Although ABCG2-mediated efflux of DXd was not directly demonstrated in H1781DSR3 cells, DXd has been reported to be a substrate of BCRP, encoded by ABCG2 (24–26). Previous preclinical studies have implicated ABC transporters in resistance to antibody–drug conjugates (ADCs), potentially through the efflux of their cytotoxic payloads (19, 27–30). For example, Murase et al. demonstrated ABCG2-mediated resistance to T-DXd in HER2-amplified gastric cancer models (30). Similarly, ABCG2 overexpression reduced the antitumor activity of datopotamab deruxtecan (Dato-DXd), a TROP2-directed ADC containing the same linker and payload as T-DXd (31), in an in vivo model using HCC827 NSCLC cells (26). However, most previous investigations have relied on preclinical models, and the clinical relevance of ABC transporters in ADC resistance remains incompletely understood. Sledge et al. investigated associations between the expression of 86 genes implicated in ADC resistance in pretreatment tumor specimens and survival outcomes in 1,144 patients with breast cancer treated with T-DXd (32). Among these genes, ABCC1, which encodes another ABC transporter, showed the strongest association with poor outcomes. Consistent with the potential involvement of multiple ABC transporters, our transcriptomic analysis demonstrated significant upregulation of both ABCG2 and ABCC1 in H1781DSR3 cells compared with parental H1781 cells (Fig. 2A). Although our functional experiments support a contribution of ABCG2 to T-DXd resistance, the potential involvement of ABCC1 cannot be excluded because its functional role was not directly investigated. These findings suggest that multiple ABC transporters may contribute to acquired T-DXd resistance, warranting further investigation of their individual and potentially cooperative roles.

Previous studies involving HER2-amplified lung and breast cancers have identified reduced HER2 copy number as a potential mechanism of acquired T-DXd resistance (18, 33). However, the clinical significance of reduced HER2 copy number or expression in T-DXd-resistant HER2-mutant NSCLC remains unclear. Importantly, ABC transporter upregulation and HER2 loss are not necessarily mutually exclusive and may coexist within resistant tumors, contributing to resistance through distinct mechanisms. Further investigations using paired clinical specimens and patient-derived models are needed to determine the relative contributions and potential coexistence of these mechanisms.

In the present study, patient-derived organoids established from T-DXd-resistant tumors retained sensitivity to zongertinib, and clinical responses to zongertinib were observed in the corresponding patients. Consistent with these findings, a phase Ia/Ib trial of zongertinib in HER2-mutant NSCLC reported an objective response rate of 48% (95% confidence interval, 32–65%) among 31 patients previously treated with HER2-directed ADCs, including T-DXd (34). Although tumor ABCG2 expression was not evaluated in that trial, our findings suggest that zongertinib may retain activity in tumors with ABCG2-associated T-DXd resistance. Similarly, Nilsson et al. reported that HER2-mutant NSCLC cell lines with acquired resistance to T-DXd remained sensitive to HER2 tyrosine kinase inhibitors (TKIs), including zongertinib and poziotinib (19). In our resistant cell model, HER2 and downstream signaling remained detectable, and zongertinib inhibited HER2 phosphorylation and exerted antitumor activity. These observations suggest that ABCG2-associated resistance to the cytotoxic payload of T-DXd does not necessarily eliminate dependence on HER2 signaling, providing a rationale for HER2-targeted TKI therapy after T-DXd resistance. However, the extent to which HER2 signaling remains essential for tumor survival after the acquisition of resistance requires further investigation.

Previous studies have reported lower ABCG2 expression in NSCLC tumors than in adjacent normal tissues (35), a pattern also observed in our pretreatment specimens. Nevertheless, some tumors exhibited relatively high ABCG2 expression before T-DXd treatment, raising the possibility that baseline ABCG2 expression may influence treatment sensitivity. However, the clinical association between pretreatment ABCG2 expression and T-DXd efficacy remains uncertain because of the limited sample size and exploratory nature of our analysis. These findings also raise the possibility that combining T-DXd with a HER2-targeted TKI could help overcome or delay resistance. Nevertheless, the efficacy and safety of such combinations were not directly evaluated in this study and require further preclinical and clinical investigation.

Increased ABCG2 expression was observed in five of six paired tumor specimens obtained before T-DXd treatment and after the development of acquired resistance. However, the small number of paired specimens precludes reliable estimation of its prevalence. As ADC development expands to include diverse target antigens (36), many emerging agents continue to incorporate topoisomerase I inhibitor payloads (37). Dato-DXd, for example, has demonstrated promising clinical activity in NSCLC, particularly in tumors harboring actionable genomic alterations, but shares the same cytotoxic payload as T-DXd (31, 38). Because ABCG2 can transport DXd, its upregulation may potentially contribute to cross-resistance between ADCs containing the same payload. However, cross-resistance between T-DXd and Dato-DXd was not directly investigated in this study, and this possibility requires experimental and clinical validation.

The relevance of ABCG2 to T-DXd resistance in other cancer types also remains to be established. In our exploratory analysis of four patients with HER2-positive breast cancer who developed resistance to T-DXd, increased BCRP expression was observed in post-treatment tumor specimens (Supplementary Fig. S8). Notably, breast cancer Case 4 also exhibited a decrease in HER2 expression from IHC 3 + before treatment to IHC 0 after resistance development. This observation suggests that HER2 loss and ABCG2

upregulation may coexist in resistant tumors, although their individual contributions to resistance cannot be determined from these clinical observations. Together, these findings highlight the potential heterogeneity of acquired T-DXd resistance and the need to evaluate ABCG2 alongside other resistance-associated alterations across different tumor types.

Several limitations of this study should be acknowledged. First, the clinical analysis included 31 tumor specimens from patients with HER2-mutant NSCLC, and the number of paired pre- and post-treatment specimens was particularly limited. Accordingly, the findings may not fully capture the heterogeneity of resistance mechanisms across patients with different genetic backgrounds. Second, the retrospective study design, post hoc definition of BCRP expression categories, and lack of formal inter-reader agreement assessment limit the interpretation of the clinical biomarker findings. Therefore, the clinical biomarker findings should be regarded as exploratory and require validation in larger independent cohorts using standardized assessment methods. Third, individual tumor biopsies represent only a limited portion of the tumor, and intratumoral and interlesional heterogeneity in ABCG2 expression could not be comprehensively evaluated. Previous studies have demonstrated heterogeneous ABCG2 expression in surgically resected tumors (39). Analysis of multiple tumor regions or metastatic sites may therefore be necessary to characterize the spatial heterogeneity of resistance mechanisms. Finally, although functional inhibition and knockdown experiments support the involvement of ABCG2 in T-DXd resistance, direct measurement of ABCG2-mediated DXd efflux was not performed. The potential contributions of other transporters, including ABCC1, and additional resistance mechanisms also remain unresolved.

The role of ABCG2 in resistance to topoisomerase I inhibitors, including camptothecin and SN-38, has been recognized for more than two decades (40). Our findings extend these observations to T-DXd-resistant HER2-mutant NSCLC by integrating experimental models with analyses of clinical specimens and patient-derived organoids. Collectively, the results suggest that ABCG2 upregulation may contribute to acquired T-DXd resistance in a subset of HER2-mutant NSCLC, while HER2-targeted TKIs such as zongertinib may retain antitumor activity after resistance develops. Further studies are warranted to establish the clinical utility of ABCG2 as a resistance biomarker and to optimize therapeutic strategies following T-DXd treatment.

Materials and Methods

Study design

This study integrated clinical, molecular, and preclinical analyses to investigate mechanisms of acquired resistance to trastuzumab deruxtecan (T-DXd) and evaluate potential therapeutic strategies for T-DXd-resistant HER2-mutant NSCLC. The study included assessment of ABCG2 protein expression in 31 tumor specimens from 25 patients with HER2-mutant NSCLC, genomic and transcriptomic analyses of HER2-mutant NSCLC cell lines, and functional studies using cell lines, xenograft models, and two patient-derived organoid models established from T-DXd-resistant tumors.

Cell and reagents

NCI-H1781 and NCI-H2170 human lung cancer cell lines were obtained from the American Type Culture Collection (ATCC; Manassas, VA, USA; Supplementary Fig. S9). NCI-H1781 cells have been previously reported to harbor the HER2 (ERBB2) exon 20 insertion mutation p.Gly776delinsValCys (G776delinsVC), whereas NCI-H2170 cells have been reported to exhibit HER2 amplification (18). The HER2 mutation was annotated according to the RefSeq reference transcript NM_004448.4. Cells were maintained in RPMI 1640 medium (FUJIFILM Wako Pure Chemical Corporation, Osaka, Japan) supplemented with 10% fetal bovine serum and 1% penicillin–streptomycin at 37°C in a humidified atmosphere containing 5% CO_2.

To establish T-DXd-resistant cells, parental H1781 cells were initially exposed to 1 ng/mL T-DXd, followed by stepwise increases in T-DXd concentration to a maximum of 1.0 μg/mL over 12 months. Multiple resistant clones were isolated from the pooled resistant cell population, and one clone, designated H1781DSR3, was selected for subsequent experiments. Established H1781DSR3 cells were maintained in medium containing 0.5 μg/mL T-DXd to sustain selective pressure. Before experiments, H1781DSR3 cells were cultured in T-DXd-free medium for at least 7 days, with the washout duration specified for individual experimental procedures.

T-DXd, DXd, and febuxostat were purchased from Daiichi Sankyo Co., Ltd. (Tokyo, Japan), MedChemExpress (Monmouth Junction, NJ, USA), and Selleck Chemicals (Houston, TX, USA), respectively (Supplementary Fig. S9). Zongertinib was provided by Boehringer Ingelheim International GmbH (Ingelheim am Rhein, Germany).

Cell viability assay

A total of 4×10^3 cells were seeded in a 96-well plate (Corning, Inc., NY, USA). After overnight incubation, cells were treated with the indicated concentrations of DXd for 72 h. Cell viability was assessed using the CellTiter-Glo Luminescent Cell Viability Assay (Promega, Madison, WI, USA, RRID: SCR_001356) according to the manufacturer's instructions. Luminescence was measured using a microplate reader (ARVO MX 1420; PerkinElmer, Shelton, CT, USA). Cell viability was expressed as a percentage of the luminescence measured in untreated control cells. Half-maximal inhibitory concentrations (IC50 values) were estimated by nonlinear regression analysis of concentration–response curves. H1781DSR3 cells were cultured in T-DXd-free medium for 14 days before the assay.

High-density cell growth assay

Cells were seeded in 6-well plates at a density of 3.0×10^5 cells per well. After 24 h, cells were treated with 1.0 μg/mL T-DXd, 10 μM febuxostat, their combination, or 100 nM zongertinib, as indicated. Febuxostat was used at 10 μM based on previous reports demonstrating its ABCG2 inhibitory activity at this concentration (41) and its minimal effect on cell growth when administered alone, as confirmed in our experiments (Supplementary Fig. S10). Drug-containing medium was replaced every 3 days. After 14 days, cells were gently washed with phosphate-buffered saline (PBS), fixed with acetic acid/methanol (1:7, v/v) for 5 min, and stained with 0.5% crystal violet for 2 h at room temperature. After removal of

excess stain, the percentage of crystal violet-stained area was quantified using ImageJ software (version 1.52a; National Institutes of Health, Bethesda, MD, USA; RRID: SCR_003070). H1781DSR3 cells were cultured in T-DXd-free medium for 14 days before the assay. The experiments were independently performed twice to assess reproducibility.

Western blotting

Cells were seeded at a density of 1 × 10^6 cells per plate and cultured overnight in RPMI 1640 medium supplemented with 10% fetal bovine serum. Cells were subsequently treated with the indicated drugs at the specified concentrations and durations before protein extraction. Proteins were transferred onto nitrocellulose membranes and probed with primary antibodies against HER2, phosphorylated HER2, AKT, phosphorylated AKT, ERK1/2, phosphorylated ERK1/2, cleaved PARP, cleaved caspase-3, ABCG2, AKR1C1/2/3, histone H2AX, phosphorylated histone H2AX (Ser139), and actin. Detailed information on the antibodies, including suppliers, catalog numbers, Research Resource Identifiers (RRIDs), and dilutions, is provided in Supplementary Fig. S9. Actin was used as a loading control where appropriate. Band intensities were quantified by densitometric analysis using ImageJ software (version 1.52a; National Institutes of Health, Bethesda, MD, USA; RRID: SCR_003070). Phosphorylated protein levels were normalized to the corresponding total protein levels where indicated, whereas other protein levels were normalized to actin.

H1781DSR3 cells were cultured in T-DXd-free medium for 14 days before the experiments.

Band intensities of histone H2AX and phosphorylated histone H2AX were quantified from exposures within the linear detection range (Supplementary Fig. S11). A total of 22.5 μg of protein was loaded per lane, and exposure times of 10 s and 5 s were used for phosphorylated and total histone H2AX, respectively. Quantification was performed using independently obtained biological replicates, as indicated in the corresponding figure legends.

Original uncropped western blot images are provided in Supplementary Fig. S12.

ADC internalization detection assay

T-DXd was labeled with a pH-sensitive red fluorescent dye using an antibody internalization detection reagent (AcroBiosystems, Newark, DE, USA; Cat. No. IGG-PZF2001) according to the manufacturer's instructions. Briefly, T-DXd was incubated with the labeling reagent for 10 min at room temperature. Cells were seeded at a density of 3 × 10^5 cells per well in 6-well plates containing RPMI 1640 medium supplemented with 10% fetal bovine serum. After overnight incubation, cells were exposed to labeled 1 μg/mL T-DXd and harvested at 2, 4, 8, 16, and 24 h. Harvested cells were washed with phosphate-buffered saline (PBS), and fluorescence intensity was measured using an LSRFortessa X-20 flow cytometer (BD Biosciences, San Jose, CA, USA; RRID: SCR_025285). Flow cytometry data were analyzed using FlowJo software (FlowJo, Ashland, OR, USA; RRID: SCR_008520). H1781DSR3 cells were cultured in T-DXd-free medium for 14 days before the assay.

Microarray and pathway analyses

Gene expression profiling was performed using the Affymetrix Clariom S Human Array (Cat. No. 902926; Thermo Fisher Scientific, Waltham, MA, USA) with two independent biological replicates for each cell line (parental H1781 and H1781DSR3). H1781DSR3 cells were cultured in T-DXd-free medium for 14 days before RNA extraction. Total RNA was extracted using the RNeasy Mini Kit (Qiagen, Hilden, Germany; Cat. No. 74104) according to the manufacturer's instructions. Microarray experiments were performed according to the manufacturer's protocol. Gene expression data were analyzed using Transcriptome Analysis Console software (version 4.0.3; Thermo Fisher Scientific; RRID:SCR_016519). Differentially expressed transcripts were defined by a fold change ≥ 2 or ≤ − 2 and an unadjusted P value < 0.05, calculated using analysis of variance (ANOVA). False discovery rate (FDR)-adjusted P values were also calculated to account for multiple testing. Pathway enrichment analysis was performed using WikiPathways through Transcriptome Analysis Console software, and pathways were ranked according to the Significance Score calculated by the software. The pathway analysis was considered exploratory and was not interpreted as direct evidence of functional pathway activation.

Next-generation sequencing (NGS)

Targeted next-generation sequencing was performed using the Oncomine Tumor Mutation Load Assay (Thermo Fisher Scientific, Waltham, MA, USA; Cat. No. A37909), an amplicon-based assay covering 409 cancer-related genes across approximately 1.7 Mb of genomic DNA, including 1.2 Mb of exonic regions. Library preparation and sequencing were performed according to the manufacturer's instructions. Sequencing data were processed using Torrent Suite software (version 5.12) and analyzed using Ion Reporter software (version 5.18; Thermo Fisher Scientific). Sequence variants were filtered using a minimum sequencing depth of 50 reads and a variant allele frequency of ≥ 2%. Variant calls were manually reviewed using Integrative Genomics Viewer (IGV; Broad Institute, Cambridge, MA, USA). Copy number alterations were assessed using Ion Reporter, with copy number gain defined as an estimated copy number ≥ 5.

To assess the reliability of negative mutation findings, sequencing quality metrics and coverage of the targeted ERBB2 and TOP1 regions were evaluated in both parental H1781 and H1781DSR3 cells. Sequencing performance was assessed using mapped read counts, on-target rates, mean sequencing depth, and coverage uniformity. Region-specific sequencing depth was examined to identify areas of insufficient coverage that could limit variant detection. Detailed sequencing quality metrics and coverage data are provided in Supplementary Fig.S1. Negative mutation findings were interpreted within the limits of the targeted regions, sequencing coverage, and variant detection thresholds of the assay. Mutations in regions with insufficient coverage, variants below the detection threshold, and alterations not detectable by this targeted sequencing assay could not be excluded.

siRNA knockdown

ABCG2 expression was silenced in T-DXd-resistant H1781DSR3 cells using 100nM ABCG2-targeting siRNA pool (ON-TARGETplus SMARTpool; Dharmacon, GE Healthcare Life Sciences, Little Chalfont, UK). Scrambled and non-targeting control siRNAs were used as negative controls. Cells were seeded in 6-well

plates at 50–60% confluence and transfected using Lipofectamine RNAiMAX (Thermo Fisher Scientific, Waltham, MA, USA; Cat. No. 13778150) according to the manufacturer's instructions. For western blotting, cells were harvested 72 h after transfection to assess ABCG2 knockdown efficiency. For DXd or T-DXd sensitivity assays, cells were transferred to 96-well plates 24 h after siRNA transfection. After an additional 24 h, cells were treated with the indicated concentrations of DXd for 72 h, and cell viability was assessed using the CellTiter-Glo assay, as described above. H1781DSR3 cells were cultured in T-DXd-free medium for 14 days before transfection.

In vivo growth inhibition assay

All animal experiments were conducted in accordance with the Recommendations for Handling of Laboratory Animals for Biomedical Research established by the Committee on Safety and Ethical Handling Regulations for Laboratory Animal Experiments of Kindai University. The study protocol was approved by the Animal Ethics Committee of Kindai University. H1781 or H1781DSR3 cells (1×10^7 cells/mouse) mixed with Matrigel Basement Membrane Matrix (Cat. No. 354234; Corning Incorporated, Corning, NY, USA) were subcutaneously injected into the right flank of female BALB/cAJcl-nu/nu mice (RRID:IMSR_JCL:JCL; CLEA Japan, Tokyo, Japan). Once the tumors reached a volume of approximately 0.2 cm^3, the mice were randomly allocated to treatment groups (n = 10 per group). Mice received a single intraperitoneal injection of PBS (200 µL; vehicle control) or T-DXd (3 mg/kg body weight in 200 µL PBS) on day 1. Zongertinib (10 mg/kg in 100 µL 0.5% hydroxypropyl methylcellulose) was administered orally (p.o.) once daily on weekdays (five times per week), starting on day 1 and continuing until the final tumor-volume measurement. Tumor volume and body weight were measured twice weekly. Tumor volume was calculated using the formula: volume = (length × $width^2$)/2. Mice were euthanized if tumors developed necrosis or reached a volume of 2.0 cm^3. The vehicle control and T-DXd-treated groups were shared between the experiments presented in Figs. 2K/L and 5E/F. Thus, the same animals and their corresponding tumor-volume measurements were used in both analyses. H1781DSR3 cells were maintained in T-DXd-free medium for two weeks before inoculation into mice.

Establishment of ABCG2-overexpressing cell lines

The pPB[Exp]-Puro-CAG-3xFLAG/ABCG2[NM_001348985.1]-IRES-EGFP (VectorBuilder Inc, Kanagawa, Japan) vector was transfected into H1781 cells and H2170 cells together with a plasmid encoding the PiggyBac transposase with the use of a NEPA21 electroporation system (Nepagene, Chiba, Japan). These cells were cultured in DMEM supplemented 10% FBS and puromycin (1 µg/mL) for 10 days.

Absolute quantification of cell-surface HER2 expression

A total of 5×10^5 cells were stained with an anti-HER2 antibody (BioLegend, Cat. No. 324401), with mouse IgG1 (BioLegend, Cat. No. 401401) used as an isotype control. Cell-surface HER2 expression was quantified using QIFIKIT (Dako, Glostrup, Denmark; Cat. No. K0078) according to the manufacturer's instructions. Cells and calibration beads were stained with an FITC-conjugated secondary antibody and analyzed using an LSRFortessa X-20 flow cytometer (BD Biosciences). Mean fluorescence intensity (MFI) was determined using FlowJo software (BD Biosciences). A calibration curve was generated by

linear regression of bead MFI against the corresponding antibody-binding capacity (ABC) using Microsoft Excel version 16.0 (Microsoft, Redmond, WA, USA; RRID:SCR_016137). The number of HER2 antibody-binding sites per cell was calculated from the calibration curve. H1781DSR3 cells were maintained in T-DXd-free medium for two weeks before the assay.

Immunohistochemical analysis of BCRP/ABCG2

H1781 and H1781DSR3 xenograft tumors and samples from patients with HER2-mutant NSCLC who received T-DXd were formalin-fixed and paraffin-embedded, and tissue sections were used for immunohistochemical (IHC) analysis. The 3-μm-thick sections on slides were subjected to heat-induced epitope retrieval and incubated with mouse anti-BCRP/ABCG2 (Abcam, Cambridge, UK, Cat# ab3380, RRID: AB_303758). The primary antibody was detected using the DAKO REAL Envision detection system with the Peroxidase/DAB and Rabbit/Mouse horseradish peroxidase kits (Agilent, Cat# K5007, RRID: AB_2888627). Sections were counterstained with hematoxylin. The BCRP (ABCG2) staining pattern was scored as 0, 1+, 2+, or 3 + as follows: 0, no membranous staining or faint, incomplete membranous staining in ≤ 10% of tumor cells; 1+, > 10% tumor cells with faint, incomplete membranous staining; 2+, > 10% tumor cells with weak-to-moderate complete membranous staining or ≤ 10% tumor cells with intense complete membranous staining; and 3+, > 10% tumor cells with intense complete membranous staining (Fig. 3B). IHC scores were independently assessed by one pathologist and one researcher, blinded to clinical outcomes. Discrepant scores were resolved by consensus. Interobserver agreement was not formally quantified. For exploratory clinical analyses, tumors were categorized as having low (scores 0 and 1+) or high (scores 2 + and 3+) BCRP expression using a post hoc-defined cutoff.

Establishment of patient-derived NSCLC organoids from malignant pleural effusion and bronchoscopy biopsy specimens

Malignant pleural effusion samples and bronchoscopy biopsy specimens were obtained from patients with T-DXd-resistant HER2-mutant NSCLC, with written informed consent and institutional review board approval. Approximately 100 mL of the pleural effusion was collected and processed within 30 min of drainage. After washing with phosphate-buffered saline, isolated cells were resuspended in growth factor-reduced basement membrane extract (BME/Matrigel; Corning, Inc., NY, USA, RRID: AB_257087) and seeded as 50 μL domes, each containing 1.0×10^5 cells, onto prewarmed 24-well plates. Bronchoscopic biopsy specimens from primary tumors were transported to the laboratory on ice in Advanced Dulbecco's modified Eagle medium (DMEM) within 30 min of collection. After mincing into fragments < 1 mm^3 under sterile conditions, the specimens were digested for 30–60 min using 1.5 mg/mL collagenase II (Gibco, Thermo Fisher Scientific, Cat# 17101-015) and 2 mg/mL dispase type II (Gibco, Thermo Fisher Scientific, Cat# 17105-041, RRID: AB_2340462). The digest was filtered through a cell strainer (Corning, Inc.), and the filtrate was centrifuged at 300 × *g* for 5 min. The pellet was washed twice with transport medium and embedded in 50 μL Matrigel on a prewarmed 24-well plate. After warming at 37°C for 3–5 min, lung cancer organoid culture medium was added around the dome of each

well. The composition of the basal medium and supplements used for patient-derived organoid culture is provided in Supplementary Fig. S9. The ROCK inhibitor Y-27632 (5 μM; FUJIFILM Wako Pure Chemical Corporation, Cat. No. 036-24023) was added during the initial culture period to enhance cell survival. Organoids were expanded for at least five passages before use, and all experiments were performed using organoids at passages below 10.

Drug sensitivity assays using PDOs

For drug sensitivity assays, established patient-derived organoids (PDOs) were replated in Matrigel domes as described above and cultured until stable growth was observed. Organoids were then treated with the indicated anticancer agents for 13–18 days. In longitudinal growth assays, five or six individual organoids within a single well per treatment condition were monitored over time. Organoid diameters were measured at the indicated time points using a BZ-X710 All-in-One Fluorescence Microscope (KEYENCE Corporation, Osaka, Japan). Data are presented as the mean ± SEM of the six tracked organoids. No inferential statistical comparisons were performed because organoids within the same well were not independent experimental replicates.

For independent-well assays, six separate wells per treatment condition were used, with one organoid per well. Growth rate (%) was calculated for each organoid as the diameter at the indicated endpoint divided by its diameter at baseline (before treatment), multiplied by 100. Statistical comparisons were performed using independent wells as the experimental units.

Statistical analysis

Dose–response curves were fitted by nonlinear regression using GraphPad Prism version 10.4.2 (GraphPad Software, Boston, MA, USA; RRID: SCR_002798), and half-maximal inhibitory concentration (IC50) values were estimated from the fitted curves. Statistical analyses were performed using SPSS version 22.0 (IBM Corp., Armonk, NY, USA; RRID: SCR_016479) and GraphPad Prism, as appropriate. Comparisons between two independent groups were performed using unpaired Student's t-tests, whereas comparisons of paired BCRP immunohistochemical scores before and after T-DXd treatment were performed using the Wilcoxon signed-rank test. Associations between categorical variables, including objective response and pretreatment BCRP expression, were assessed using Fisher's exact test. Comparisons among multiple independent treatment groups were performed using one-way analysis of variance (ANOVA), followed by Tukey's multiple-comparison test, where applicable. For xenograft experiments, statistical comparisons of tumor volumes were performed at the final measurement time point. In longitudinal patient-derived organoid assays, six organoids within a single well per treatment condition were monitored descriptively without inferential statistical testing. For independent-well organoid assays, each well was treated as an independent experimental unit, and treatment groups were compared using one-way ANOVA followed by Tukey's multiple-comparison test.

Tumor responses were retrospectively assessed according to Response Evaluation Criteria in Solid Tumors (RECIST), version 1.1 (42). Objective response rate was defined as the proportion of patients

achieving a complete response (CR) or partial response (PR). Progression-free survival (PFS) was defined as the time from initiation of T-DXd treatment to disease progression according to RECIST version 1.1 or death from any cause, whichever occurred first. Patients without documented progression or death were censored at the date of their last disease assessment. PFS was estimated using the Kaplan–Meier method, and differences between groups were assessed using the log-rank test. Hazard ratios (HRs) and 95% confidence intervals (CIs) were estimated using univariable Cox proportional hazards regression. All statistical tests were two-sided, and $P < 0.05$ was considered statistically significant. Graphs were generated using GraphPad Prism.

Patients

This study collected clinical background information for patients with lung adenocarcinoma harboring HER2 gene mutations as well as CT images from before and after T-DXd treatment. This study was approved by the Institutional Review Boards of Kindai Hospital, Kansai Medical University Hospital, Osaka Medical and Pharmaceutical University Hospital, Kagoshima University Hospital, and Kyushu University Hospital. Written informed consent was obtained from all participants.

Study approval

This study was approved by the Medical Ethics Review Committee of Kindai Hospital (approval number: R07-037) and was conducted in accordance with the Declaration of Helsinki. The committee also approved the use of patient specimens for immunohistochemistry, as well as the establishment of patient-derived organoids and their use in drug sensitivity assays. Written informed consent was obtained from all patients.

Data availability

The raw and processed microarray data generated in this study have been deposited in the NCBI Gene Expression Omnibus (GEO) database under accession number GSE350378 (https://www.ncbi.nlm.nih.gov/geo/query/acc.cgi?acc=GSE350378). Numerical source data underlying the quantitative figures are provided in the accompanying Source Data files.

Patient-level clinical and genomic data are not publicly available due to patient privacy considerations and ethical restrictions associated with the retrospective study conducted under an opt-out consent procedure. Requests for access to these data may be directed to the corresponding author and will be evaluated in accordance with institutional ethical requirements, applicable data protection regulations, and the scope of the approved research protocol.

Declarations

Competing Interests

Y. Kawanaka reports receiving research funding from Nippon Boehringer Ingelheim Co., Ltd. K. Yonesaka reports receiving research funding from Nippon Boehringer Ingelheim Co., Ltd. and Boehringer Ingelheim International GmbH; grants from Daiichi Sankyo Co., Ltd.; honoraria from Daiichi Sankyo Co., Ltd., AstraZeneca K.K., Chugai Pharmaceutical Co., Ltd., Pfizer Japan Inc. and Amgen Inc.; patents planned and issued from Daiichi Sankyo Co., Ltd. T. Kurosaki reports receiving research funding from Nippon Boehringer Ingelheim Co., Ltd.; grants from Chugai Pharmaceutical Co., Ltd. S. Suzuki reports receiving research funding from Nippon Boehringer Ingelheim Co., Ltd.; grants from Boehringer Ingelheim Co., Ltd. H. Kanemura reports receiving grants from Chugai Pharmaceutical Co., Ltd., Takeda Pharmaceutical Co., Ltd.; honoraria from Chugai Pharmaceutical Co., Ltd., AstraZeneca K.K., Daiichi Sankyo Co., Ltd., MSD K.K. and Novartis Pharma K.K. S. Watanabe reports receiving honoraria from Daiichi Sankyo Co., Ltd., Chugai Pharmaceutical Co., Ltd., MSD K.K., Eli Lilly Japan K.K., Kyowa Kirin Co., Ltd., and Eisai Co., Ltd., and Pfizer K.K., and serving on an advisory board for Daiichi Sankyo Co., Ltd. T. Takahama reports receiving honoraria from Chugai Pharmaceutical Co., Ltd. and AstraZeneca K.K. J. Tanizaki reports receiving honoraria from AstraZeneca K.K., AbbVie GK., Amgen Inc., Boehringer Ingelheim Japan Inc., Bristol-Myers Squibb Co. Ltd., Chugai Pharmaceutical Co., Ltd., Daiichi Sankyo Co., Ltd., Eli Lilly Japan K.K., Janssen Pharmaceutical K.K., Johnson & Johnson, MSD K.K., Ono Pharmaceutical Co., Ltd., Pfizer Japan Inc., Taiho Pharmaceutical Co. Ltd. and Takeda Pharmaceuticals, and serving on an advisory board for AstraZeneca K.K., Chugai Pharmaceutical Co., Ltd., Janssen Pharmaceutical K.K. and Pfizer Japan Inc. Kaoru Tanaka reports receiving honoraria from AstraZeneca K.K., Merck Biopharma Co., Ltd., Eisai Co., Ltd., Bristol-Myers Squibb K.K., Ono Pharmaceutical Co., Ltd., MSD K.K., Chugai Pharmaceutical Co., Ltd., Takeda Pharmaceutical Co., Ltd., Taiho Pharmaceutical Co., Ltd., Kyowa Kirin Co., Ltd. and Novartis Pharma K.K. K. Sakai reports receiving honoraria from Qiagen, Inc., Takeda Pharmaceutical Co., Ltd., Nippon Kayaku Co., Ltd., and Life Technologies Japan Ltd. Y. Tamura reports receiving honoraria from MSD K.K., Chugai Pharmaceutical Co., Ltd., AstraZeneca K.K., Ono Pharmaceutical Co., Ltd., and Boehringer Ingelheim Japan Inc.; grants from AbbVie Inc., Ono Pharmaceutical Co. Ltd., and Shanghai Junshi Biosciences Co., Ltd. E. Iwama reports personal fees from AstraZeneca and Chugai Pharmaceutical. Kentaro Tanaka reports serving on the advisory council with AstraZeneca and Pfizer; speaker's bureau with AstraZeneca, Bristol Myers Squibb, Chugai Pharmaceutical, Merck, Merck Sharp & Dohme, and Ono Pharmaceutical. Y. Fujisaka reports receiving honoraria from Eli Lilly Japan K.K., AstraZeneca, Chugai Pharmaceutical Co., Ltd., Pfizer Japan Inc., Ono Pharmaceutical Co., Ltd., Daiichi Sankyo Co., Ltd, and Taiho Pharmaceutical Co. Ltd.; grants from Summit Therapeutics Sub, Taiho Pharmaceutical Co., Ltd., MSD K.K., Daiichi Sankyo Co., Ltd., Bristol-Myers Squibb Co., Ltd., Genmab K.K., Pfizer Japan Inc., Kyowa Kirin Co., Ltd., AbbVie GK, and Ono Pharmaceutical Co., Ltd. T. Kurata reports personal fees from MSD, Ono Pharmaceutical, Bristol-Myers Squibb, AstraZeneca, Chugai Pharma, and Janssen Pharmaceuticals, and grants from MSD, Daiichi Sankyo, Chugai Pharma, Amgen, Janssen Pharmaceuticals, BeOne, SUMMIT, and Regeneron. I. Okamoto reports receiving grants from Chugai Pharmaceutical, AstraZeneca, Taiho Pharmaceutical, Boehringer Ingelheim, Ono Pharmaceutical, MSD, Eli Lilly, Astellas, Bristol Myers Squibb, Novartis, Pfizer, and AbbVie; consulting fees from AstraZeneca, Bristol Myers Squibb, and AbbVie; and personal fees from AstraZeneca, Taiho Pharmaceutical, Boehringer Ingelheim, Chugai Pharmaceutical, Ono Pharmaceutical, MSD, Eli Lilly, Bristol-Myers Squibb,

Novartis, and Pfizer. K. Nishio reports receiving grants from West Japan Oncology Group, Hitachi Ltd., Otsuka Pharmaceutical Co., Ltd., Thoracic Oncology Research Group, Eli Lilly Japan K.K., Okayama University, Japan Breast Cancer Research Group, Nippon Boehringer Ingelheim Co., Ltd., and Kyushu Study Group of Clinical Cancer; consulting fees from SymBio Pharmaceuticals Ltd., Eli Lilly Japan K.K., and Otsuka Pharmaceutical Co., Ltd.; and honoraria from Chugai Pharmaceutical Co., Ltd., MSD K.K., Guardant Health, Janssen Pharmaceutical K.K., Eli Lilly Japan K.K., AstraZeneca K.K., Nichirei Biosciences Inc., and Maruho Co., Ltd. H. Hayashi reports grants from IQVIA Services JAPAN K.K., SYNEOS HEALTH CLINICAL K.K., EPS Corporation., Nippon Kayaku Co., Ltd., Takeda Pharmaceutical Co., Ltd., MSD K.K., Amgen Inc., Taiho Pharmaceutical Co., Ltd., Bristol Myers Squibb Company, Janssen Pharmaceutical K.K., CMIC CO., Ltd., Pfizer R&D Japan G.K., Labcorp Development Japan K.K., Kobayashi Pharmaceutical Co., Ltd., Pfizer Japan Inc., AbbVie Inc., A2 Healthcare Corp., Eisai Co., Ltd., EP-CRSU CO., LTD., Shionogi & Co., Ltd., Otsuka Pharmaceutical Co., Ltd., GlaxoSmithKline K.K., Sanofi K.K., Chugai Pharmaceutical Co., Ltd., Nippon Boehringer Ingelheim Co., Ltd., SRL Medisearch Inc., PRA Health Sciences Inc., Astellas Pharma Inc., Ascent Development Services, Eisai Inc., Bayer Yakuhin, Ltd., AstraZeneca K.K., Daiichi Sankyo Co., Ltd., Novartis Pharma K.K., Eli Lilly Japan K.K., Medpace Japan K.K., Japanese Gastric Cancer Association, Clinical Research Support Center Kyushu, Japan Clinical Cancer Research Organization, Merck Biopharma Co., Ltd, Kyowa Kirin Co., Ltd., Thoracic Oncology Research Group, West Japan Oncology Group, Comprehensive Support Project for Oncological Research of Breast Cancer, Mochida Pharmaceutical Co., Ltd., MSD K.K., Sysmex Corporation., Public Health Research Foundation., ICON Japan K.K. and PPD-SNBL K.K.; honoraria from Ono Pharmaceutical Co., Ltd., Daiichi Sankyo Co., Ltd., AstraZeneca K.K., Chugai Pharmaceutical Co., Ltd., Eli Lilly Japan K.K., MSD K.K., Pfizer Japan Inc., Nippon Boehringer Ingelheim Co., Ltd., Guardant Health Japan Corp., Merck Biopharma Co., Ltd., 3H Clinical Trial Inc., Novartis Pharma K.K., Bristol Myers Squibb Company, Amgen Inc., Sysmex Corporation, Takeda Pharmaceutical Co., Ltd. and Janssen Pharmaceutical K.K., AbbVie Inc., Kyowa Kirin Co., Ltd., Reno. Medical K.K., Nippon Kayaku Co., Ltd., Hisamitsu Pharmaceutical Co., Inc., Novocure K.K., Eisai Co., Ltd., Care Net, Inc., Taiho Pharmaceutical Co., Ltd., 3H Clinical Trial Inc., Ishiyaku Publishers, Inc. and Medical Review Co., Ltd.; participation in a data safety monitoring board or advisory board for Bristol Myers Squibb Company, Chugai Pharmaceutical Co., Ltd., AstraZeneca K.K., Janssen Pharmaceutical K.K., AbbVie Inc., Novocure K.K., and Daiichi Sankyo Co., Ltd. The other authors declare no competing interests.

Conflict of Interest Disclosure:

Y. Kawanaka reports receiving research funding from Nippon Boehringer Ingelheim Co., Ltd. K. Yonesaka reports receiving research funding from Nippon Boehringer Ingelheim Co., Ltd. and Boehringer Ingelheim International GmbH; grants from Daiichi Sankyo Co., Ltd.; honoraria from Daiichi Sankyo Co., Ltd., AstraZeneca K.K., Chugai Pharmaceutical Co., Ltd., Pfizer Japan Inc. and Amgen Inc.; patents planned and issued from Daiichi Sankyo Co., Ltd. T. Kurosaki reports receiving research funding from Nippon Boehringer Ingelheim Co., Ltd.; grants from Chugai Pharmaceutical Co., Ltd. S. Suzuki reports receiving research funding from Nippon Boehringer Ingelheim Co., Ltd.; grants from Boehringer Ingelheim Co., Ltd.

H. Kanemura reports receiving grants from Chugai Pharmaceutical Co., Ltd., Takeda Pharmaceutical Co., Ltd.; honoraria from Chugai Pharmaceutical Co., Ltd., AstraZeneca K.K., Daiichi Sankyo Co., Ltd., MSD K.K. and Novartis Pharma K.K. S. Watanabe reports receiving honoraria from Daiichi Sankyo Co., Ltd., Chugai Pharmaceutical Co., Ltd., MSD K.K., Eli Lilly Japan K.K., Kyowa Kirin Co., Ltd., and Eisai Co., Ltd., and Pfizer K.K., and serving on an advisory board for Daiichi Sankyo Co., Ltd. T. Takahama reports receiving honoraria from Chugai Pharmaceutical Co., Ltd. and AstraZeneca K.K. J. Tanizaki reports receiving honoraria from AstraZeneca K.K., AbbVie GK., Amgen Inc., Boehringer Ingelheim Japan Inc., Bristol-Myers Squibb Co. Ltd., Chugai Pharmaceutical Co., Ltd., Daiichi Sankyo Co., Ltd., Eli Lilly Japan K.K., Janssen Pharmaceutical K.K., Johnson & Johnson, MSD K.K., Ono Pharmaceutical Co., Ltd., Pfizer Japan Inc., Taiho Pharmaceutical Co. Ltd. and Takeda Pharmaceuticals, and serving on an advisory board for AstraZeneca K.K., Chugai Pharmaceutical Co., Ltd., Janssen Pharmaceutical K.K. and Pfizer Japan Inc. Kaoru Tanaka reports receiving honoraria from AstraZeneca K.K., Merck Biopharma Co., Ltd., Eisai Co., Ltd., Bristol-Myers Squibb K.K., Ono Pharmaceutical Co., Ltd., MSD K.K., Chugai Pharmaceutical Co., Ltd., Takeda Pharmaceutical Co., Ltd., Taiho Pharmaceutical Co., Ltd., Kyowa Kirin Co., Ltd. and Novartis Pharma K.K. K. Sakai reports receiving honoraria from Qiagen, Inc., Takeda Pharmaceutical Co., Ltd., Nippon Kayaku Co., Ltd., and Life Technologies Japan Ltd. Y. Tamura reports receiving honoraria from MSD K.K., Chugai Pharmaceutical Co., Ltd., AstraZeneca K.K., Ono Pharmaceutical Co., Ltd., and Boehringer Ingelheim Japan Inc.; grants from AbbVie Inc., Ono Pharmaceutical Co. Ltd., and Shanghai Junshi Biosciences Co., Ltd. E. Iwama reports personal fees from AstraZeneca and Chugai Pharmaceutical. Kentaro Tanaka reports serving on the advisory council with AstraZeneca and Pfizer; speaker's bureau with AstraZeneca, Bristol Myers Squibb, Chugai Pharmaceutical, Merck, Merck Sharp & Dohme, and Ono Pharmaceutical. Y. Fujisaka reports receiving honoraria from Eli Lilly Japan K.K., AstraZeneca, Chugai Pharmaceutical Co., Ltd., Pfizer Japan Inc., Ono Pharmaceutical Co., Ltd., Daiichi Sankyo Co., Ltd, and Taiho Pharmaceutical Co. Ltd.; grants from Summit Therapeutics Sub, Taiho Pharmaceutical Co., Ltd., MSD K.K., Daiichi Sankyo Co., Ltd., Bristol-Myers Squibb Co., Ltd., Genmab K.K., Pfizer Japan Inc., Kyowa Kirin Co., Ltd., AbbVie GK, and Ono Pharmaceutical Co., Ltd. T. Kurata reports personal fees from MSD, Ono Pharmaceutical, Bristol-Myers Squibb, AstraZeneca, Chugai Pharma, and Janssen Pharmaceuticals, and grants from MSD, Daiichi Sankyo, Chugai Pharma, Amgen, Janssen Pharmaceuticals, BeOne, SUMMIT, and Regeneron. I. Okamoto reports receiving grants from Chugai Pharmaceutical, AstraZeneca, Taiho Pharmaceutical, Boehringer Ingelheim, Ono Pharmaceutical, MSD, Eli Lilly, Astellas, Bristol Myers Squibb, Novartis, Pfizer, and AbbVie; consulting fees from AstraZeneca, Bristol Myers Squibb, and AbbVie; and personal fees from AstraZeneca, Taiho Pharmaceutical, Boehringer Ingelheim, Chugai Pharmaceutical, Ono Pharmaceutical, MSD, Eli Lilly, Bristol-Myers Squibb, Novartis, and Pfizer. K. Nishio reports receiving grants from West Japan Oncology Group, Hitachi Ltd., Otsuka Pharmaceutical Co., Ltd., Thoracic Oncology Research Group, Eli Lilly Japan K.K., Okayama University, Japan Breast Cancer Research Group, Nippon Boehringer Ingelheim Co., Ltd., and Kyushu Study Group of Clinical Cancer; consulting fees from SymBio Pharmaceuticals Ltd., Eli Lilly Japan K.K., and Otsuka Pharmaceutical Co., Ltd.; and honoraria from Chugai Pharmaceutical Co., Ltd., MSD K.K., Guardant Health, Janssen Pharmaceutical K.K., Eli Lilly Japan K.K., AstraZeneca K.K., Nichirei Biosciences Inc., and Maruho Co., Ltd. H. Hayashi reports grants from IQVIA Services JAPAN K.K.,

SYNEOS HEALTH CLINICAL K.K., EPS Corporation., Nippon Kayaku Co., Ltd., Takeda Pharmaceutical Co., Ltd., MSD K.K., Amgen Inc., Taiho Pharmaceutical Co., Ltd., Bristol Myers Squibb Company, Janssen Pharmaceutical K.K., CMIC CO., Ltd., Pfizer R&D Japan G.K., Labcorp Development Japan K.K., Kobayashi Pharmaceutical Co., Ltd., Pfizer Japan Inc., AbbVie Inc., A2 Healthcare Corp., Eisai Co., Ltd., EP-CRSU CO., LTD., Shionogi & Co., Ltd., Otsuka Pharmaceutical Co., Ltd., GlaxoSmithKline K.K., Sanofi K.K., Chugai Pharmaceutical Co., Ltd., Nippon Boehringer Ingelheim Co., Ltd., SRL Medisearch Inc., PRA Health Sciences Inc., Astellas Pharma Inc., Ascent Development Services, Eisai Inc., Bayer Yakuhin, Ltd., AstraZeneca K.K., Daiichi Sankyo Co., Ltd., Novartis Pharma K.K., Eli Lilly Japan K.K., Medpace Japan K.K., Japanese Gastric Cancer Association, Clinical Research Support Center Kyushu, Japan Clinical Cancer Research Organization, Merck Biopharma Co., Ltd, Kyowa Kirin Co., Ltd., Thoracic Oncology Research Group, West Japan Oncology Group, Comprehensive Support Project for Oncological Research of Breast Cancer, Mochida Pharmaceutical Co., Ltd., MSD K.K., Sysmex Corporation., Public Health Research Foundation., ICON Japan K.K. and PPD-SNBL K.K.; honoraria from Ono Pharmaceutical Co., Ltd., Daiichi Sankyo Co., Ltd., AstraZeneca K.K., Chugai Pharmaceutical Co., Ltd., Eli Lilly Japan K.K., MSD K.K., Pfizer Japan Inc., Nippon Boehringer Ingelheim Co., Ltd., Guardant Health Japan Corp., Merck Biopharma Co., Ltd., 3H Clinical Trial Inc., Novartis Pharma K.K., Bristol Myers Squibb Company, Amgen Inc., Sysmex Corporation, Takeda Pharmaceutical Co., Ltd. and Janssen Pharmaceutical K.K., AbbVie Inc., Kyowa Kirin Co., Ltd., Reno. Medical K.K., Nippon Kayaku Co., Ltd., Hisamitsu Pharmaceutical Co., Inc., Novocure K.K., Eisai Co., Ltd., Care Net, Inc., Taiho Pharmaceutical Co., Ltd., 3H Clinical Trial Inc., Ishiyaku Publishers, Inc. and Medical Review Co., Ltd.; participation in a data safety monitoring board or advisory board for Bristol Myers Squibb Company, Chugai Pharmaceutical Co., Ltd., AstraZeneca K.K., Janssen Pharmaceutical K.K., AbbVie Inc., Novocure K.K., and Daiichi Sankyo Co., Ltd. The other authors declare no competing interests.

To. T.

Investigation, Methodology, and Writing—review and editing.

Ta. T.

Investigation, Methodology, and Writing—review and editing.

Ke. T.

Resources and Writing—review and editing.

Y. F.

Resources and Writing—review and editing.

Ta. K.

Resources and Writing—review and editing.

Author Contribution

Y. K.: Data curation, Formal analysis, Investigation, Methodology, Project administration, Resources, Validation, Visualization, and Writing—original draft.K. Y.: Conceptualization, Data curation, Funding acquisition, Investigation, Methodology, Resources, Supervision and Writing—review and editing.K. K.: Formal analysis, Investigation, Methodology, and Writing—review and editing.W. D.: Methodology, Resources and Writing—review and editing.T. K.: Methodology, Resources and Writing—review and editing.S. S.: Funding acquisition, Methodology, and Writing—review and editing.D. M.: Resources and Writing—review and editing.H. K.: Resources and Writing—review and editing.S. W.: Resources and Writing—review and editing.T. T.: Resources and Writing—review and editing.J. T.: Resources and Writing—review and editing.K. T.: Resources and Writing—review and editing.To. T.: Investigation, Methodology, and Writing—review and editing.Ta. T.: Investigation, Methodology, and Writing—review and editing.K. S.: Investigation, Methodology, and Writing—review and editing.Y. Y.: Resources and Writing—review and editing.Y. T.: Resources and Writing—review and editing.S. M.: Resources and Writing—review and editing.E. I.: Resources and Writing—review and editing.Ke. T.: Resources and Writing—review and editing. Y. F.: Resources and Writing—review and editing.Ta. K.: Resources and Writing—review and editing.I. O.: Supervision and Writing—review and editing.K. N.: Supervision and Writing—review and editing.H. H.: Conceptualization, Funding acquisition, Resources, Supervision and Writing—review and editing.

Acknowledgement

We thank Haruka Sakamoto, Yume Shinkai, and Michiko Kitano for their technical support.

Data Availability

All data generated or analysed during this study are included in this published article and its supplementary information files.

References

1. Yoon J. Oh DY. HER2-targeted therapies beyond breast cancer—an update. *Nat. Rev. Clin. Oncol.* 2024;21:675–700.
2. Cheng X. A comprehensive review of HER2 in cancer biology and therapeutics. *Genes (Basel)* 2024;15:903.

3. Waliany S, *et al.* Real-world prevalence, treatment patterns, and outcomes for patients with HER2 (ERBB2)-mutant metastatic non-small cell lung cancer, from a US-Based Clinico-genomic database. *Cancer Med.* 2024;13:e70272.
4. Kato Y, *et al.* Efficacy of immune checkpoint inhibitors plus platinum-based chemotherapy as 1st line treatment for patients with non-small cell lung cancer harboring HER2 mutations: results from LC-SCRUM-Asia. *Lung Cancer (Amsterdam, Netherlands)* 2024;197:107992.
5. Hong L, *et al.* Molecular landscape of ERBB2 alterations in 3000 advanced NSCLC patients. *NPJ Precis. Oncol.* 2024;8:217.
6. Nakada T, Sugihara K, Jikoh T, Abe Y, Agatsuma T. The latest research and development into the antibody-drug conjugate, [fam-] Trastuzumab Deruxtecan (DS-8201a), for HER2 Cancer Therapy. *Chem. Pharm. Bull (Tokyo).* 2019;67:173–85.
7. Ogitani Y, *et al.* DS-8201a, a novel HER2-targeting ADC with a novel DNA topoisomerase I inhibitor, demonstrates a promising antitumor efficacy with differentiation from T-DM1. *Clin. Cancer Res.* 2016;22:5097–108.
8. Modi S, *et al.* Trastuzumab deruxtecan in previously treated HER2-positive breast cancer. *N. Engl. J. Med.* 2020;382:610–21.
9. Shitara K, *et al.* Trastuzumab deruxtecan in previously treated HER2-positive gastric cancer. *N. Engl. J. Med.* 2020;382:2419–30.
10. Li BT, *et al.* Trastuzumab deruxtecan in HER2-mutant non-small-cell lung cancer. *N. Engl. J. Med.* 2022;386:241–51.
11. Yagisawa M, *et al.* Trastuzumab deruxtecan in advanced solid tumors with human epidermal growth factor receptor 2 amplification identified by plasma cell-free DNA testing: a multicenter, single-arm, phase II basket trial. *J. Clin. Oncol.* 2024;42:3817–25.
12. Goto K, *et al.* Trastuzumab deruxtecan in patients with HER2-mutant metastatic non-small-cell lung cancer: primary results from the randomized, phase II DESTINY-Lung02 trial. *J. Clin. Oncol.* 2023;41:4852–63.
13. Mosele F, *et al.* Trastuzumab deruxtecan in metastatic breast cancer with variable HER2 expression: the phase 2 DAISY trial. *Nat. Med.* 2023;29:2110–20.
14. Chen W, *et al.* Trastuzumab deruxtecan resistance via loss of HER2 expression and binding. *Cancer Discov.* 2026;16:235–49.
15. Tan AC, *et al.* Clinical and genomic features of HER2 Exon 20 insertion mutations and characterization of HER2 expression by immunohistochemistry in East Asian non-small-cell lung cancer. *JCO Precis. Oncol.* 2022;6:e2200278.
16. Ismail A, *et al.* HER2 alterations across solid tumors: implications for comprehensive testing. *Oncologist* 2025;30:oyaf258.
17. Heymach JV, *et al.* Zongertinib in previously treated HER2-mutant non-small-cell lung cancer. *N. Engl. J. Med* 2025;392:2321–33.

18. Kurosaki T, *et al.* Zongertinib, a novel HER2 tyrosine kinase inhibitor, maintains an anticancer activity for trastuzumab deruxtecan-resistant cancers harboring HER2-overexpression. *Int. J. Mol. Sci.* 2025;26:10515.
19. Nilsson MB, *et al.* Loss of payload sensitivity and other mechanisms of resistance to T-DXd in HER2-mutant NSCLC: implications for subsequent responsiveness to HER2 TKIs. *J. Thorac. Oncol*. 2026;2:103555.
20. Del Rio B, *et al.* Emerging targeted therapies for HER2-mutant NSCLC. *J. Thorac. Oncol*. 2026;21(10):103899.
21. Rojo de la Vega M, Chapman E, Zhang DD. NRF2 and the hallmarks of cancer. *Cancer Cell* 2018;34:21–43.
22. Chang LL, *et al.* AKR1C1 promotes non-small cell lung cancer proliferation via crosstalk between HIF-1α and metabolic reprogramming. *Transl. Oncol.* 2022;20:101421.
23. Singh A, Wu H, Zhang P, Happel C, Ma J, Biswal S. Expression of ABCG2 (BCRP) is regulated by Nrf2 in cancer cells that confers side population and chemoresistance phenotype. *Mol. Cancer Ther*. 2010;9:2365–76.
24. Roth JS, *et al.* Identification of antibody-drug conjugate payloads that are substrates of ATP-binding cassette drug efflux transporters. *Cancer Drug Resist.* 2026;9:2.
25. Nagai Y, Oitate M, Shiozawa H, Ando O. Comprehensive preclinical pharmacokinetic evaluations of trastuzumab deruxtecan (DS-8201a), a HER2-targeting antibody-drug conjugate, in cynomolgus monkeys. *Xenobiotica* 2019;49:1086–96.
26. Li WF, *et al.* OBI-992, a novel TROP2-targeted antibody-drug conjugate, demonstrates antitumor activity in multiple cancer models. *Mol. Cancer Ther.* 2025;24:163–75.
27. Loganzo F, *et al.* Tumor cells chronically treated with a trastuzumab-maytansinoid antibody-drug conjugate develop varied resistance mechanisms but respond to alternate treatments. *Mol. Cancer Ther.* 2015;14:952–63.
28. Chang CH, *et al.* Combining ABCG2 inhibitors with IMMU-132, an anti-Trop-2 antibody conjugate of SN-38, overcomes resistance to SN-38 in breast and gastric cancers. *Mol. Cancer Ther.* 2016;15:1910–9.
29. Cabaud O, *et al.* Overcoming resistance to anti-nectin-4 antibody-drug conjugate. *Mol. Cancer Ther.* 2022;21:1227–35.
30. Murase Y, *et al*. Therapeutic strategies to overcome payload resistance of trastuzumab deruxtecan in HER2-positive cancers. *Cancer Sci*. 2026;117:996–1009.
31. Okajima D, *et al.* Datopotamab deruxtecan, a novel TROP2-directed antibody–drug conjugate, demonstrates potent antitumor activity by efficient drug delivery to tumor cells. *Mol. Cancer Ther.* 2021;20:2329–40.
32. Sledge GW, *et al.* Mechanisms of resistance to trastuzumab deruxtecan in breast cancer elucidated by multi-omic molecular profiling. *npj Breast Cancer* 2025;12:1.

33. Gouda MA, *et al.* Human epidermal growth factor receptor 2 loss following treatment with trastuzumab deruxtecan in patients with metastatic breast cancer. *Clin. Cancer Res.* 2025;31:1268–74.
34. Heymach JV, *et al.* Zongertinib in patients with pretreated HER2-mutant advanced NSCLC: Beamion LUNG-1. *Cancer Res*. 2025;85:CT050.
35. Jeleń A, Żebrowska-Nawrocka M, Łochowski M, Szmajda-Krygier D, Balcerczak E. ABCG2 gene expression in non-small cell lung cancer. *Biomedicines* 2024;12:2394.
36. Tsuchikama K, Anami Y, Ha SYY, Yamazaki CM. Exploring the next generation of antibody–drug conjugates. *Nat. Rev. Clin. Oncol.* 2024;21:203–23.
37. Colombo R, Tarantino P, Rich JR, LoRusso PM, de Vries EGE. The journey of antibody-drug conjugates: lessons learned from 40 years of development. *Cancer Discov.* 2024;14:2089–108.
38. Sands J, *et al.* Datopotamab deruxtecan in advanced or metastatic non–small cell lung cancer with actionable genomic alterations: results from the phase II TROPION-Lung05 study. *J. Clin. Oncol.* 2025;43:1254–65.
39. Herpel E, *et al.* The cancer stem cell antigens CD133, BCRP1/ABCG2 and CD117/c-KIT are not associated with prognosis in resected early-stage non-small cell lung cancer. *Anticancer Res.* 2011;31:4491–500.
40. Sajid A, Rahman H, Ambudkar SV. Advances in the structure, mechanism and targeting of chemoresistance-linked ABC transporters. *Nat. Rev. Cancer* 2023;23:762–79.
41. Kawashima K, Ikemura K, Takemura M, Toyozumi Y, Okuda M. Febuxostat enhances the efficacy of dasatinib by inhibiting ATP-binding cassette subfamily G member 2 (ABCG2) in chronic myeloid leukemia cells. *Biomed. Pharmacother*. 2024;181:117709.
42. Eisenhauer EA, *et al.* New response evaluation criteria in solid tumours: Revised RECIST guideline (version 1.1). *Eur. J. Cancer* 2009;45(2):228–247.

Figures

Fig 1

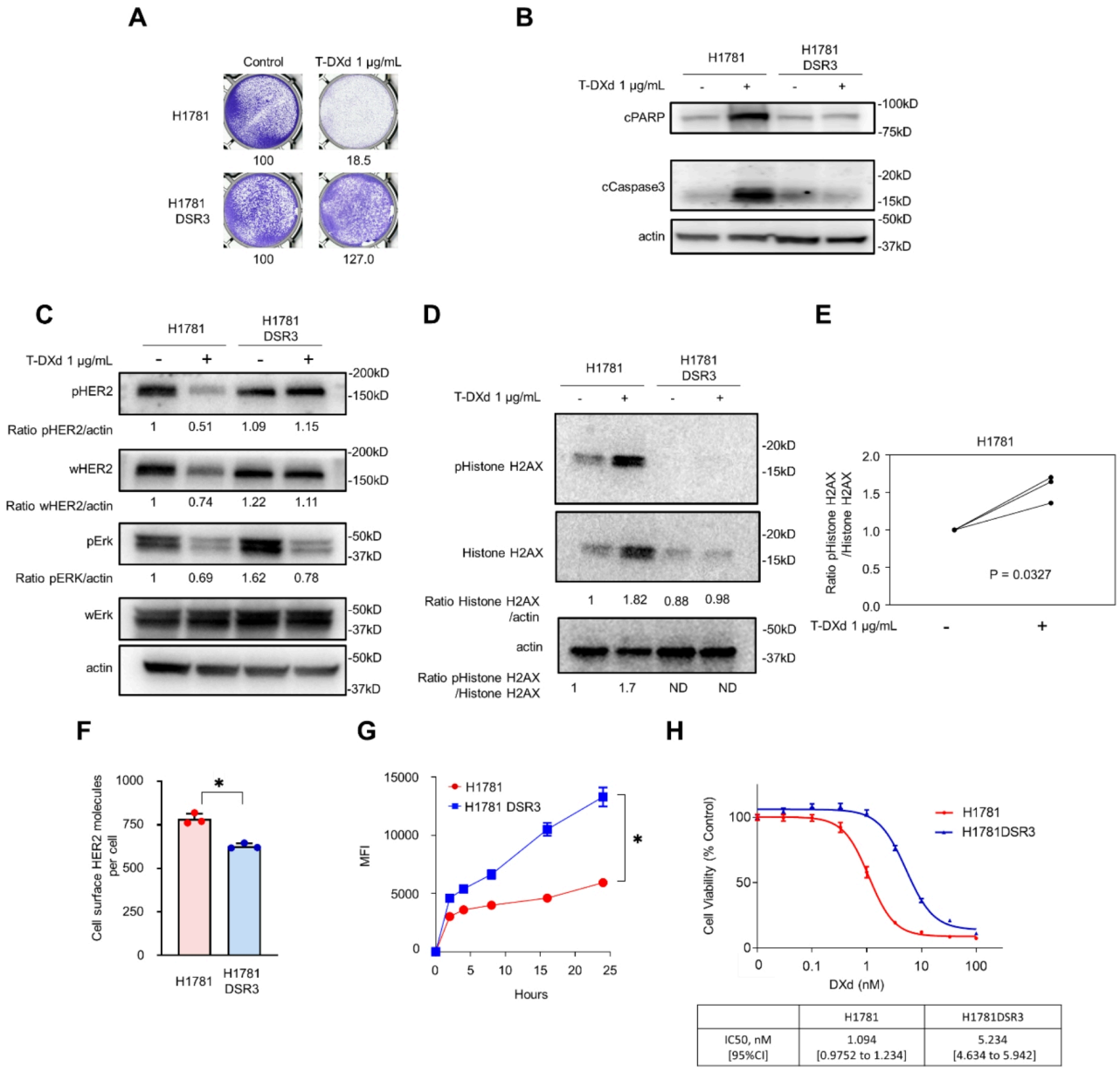


Figure 1

Characterization of acquired T-DXd resistance in H1781DSR3 cells.

(A) High-density cell growth assays were performed using HER2-mutant H1781 cells and the DSR3 clone treated with or without T-DXd (1 μg/mL) for 14 days. Crystal violet-stained areas were quantified using ImageJ. The experiment was performed twice independently, and representative results are shown.

(B–D) H1781 and DSR3 cells were treated withor without T-DXd (1 μg/mL) for 72 h. Protein expression and phosphorylation were assessed by western blotting. Band intensities were quantified by

densitometry and normalized to indicated reference proteins.

(E) Quantification of phosphorylated histone H2AX relative to total histone H2AX in H1781 cells treated with or without T-DXd (1 μg/mL) for 72 h. Band intensities were quantified by densitometry, and phosphorylated histone H2AX/total H2AX ratios were calculated. Data are obtained from three independent experiments. Statistical significance was assessed using a paired t-test.

(F) Cell-surface HER2 expression in H1781 and H1781DSR3 cells was quantified by flow cytometry. Data are presented as the mean number of HER2 molecules per cell ± SD from three replicatedexperiments. Statistical significance was assessed using an unpaired t-test.

(G) Delivery of T-DXd to acidic intracellular compartments was evaluated using pHrodo-labeled T-DXd. H1781 and H1781DSR3 cells were incubated with pHrodo-labeled T-DXd (1 μg/mL) for the indicated durations, and fluorescence intensity was measured by flow cytometry. Data are presented as MFI ± SD from three replicated experiments. Statistical significance was assessed using two-way ANOVA.

(H) Dose–response curves for DXd in parental H1781 and H1781DSR3 cells. Cells were treated with the indicated concentrations of DXd for 72 h, and cell viability was normalized to that of untreated controls. Data are presented as the mean with SEM from six replicates. Dose–response curves were fitted using nonlinear regression. Half-maximal inhibitory concentration (IC50) values and their corresponding 95% CIs are indicated in the figure. The experiment was performed twice independently, and representative results are shown.

*$p < 0.05$. T-DXd, trastuzumab deruxtecan; HER2, human epidermal growth factor receptor 2; DXd, deruxtecan; MFI, mean fluorescence intensity; SD, standard deviation; SEM, standard error of the mean, CI, confidence interval; ANOVA, analysis of variance.

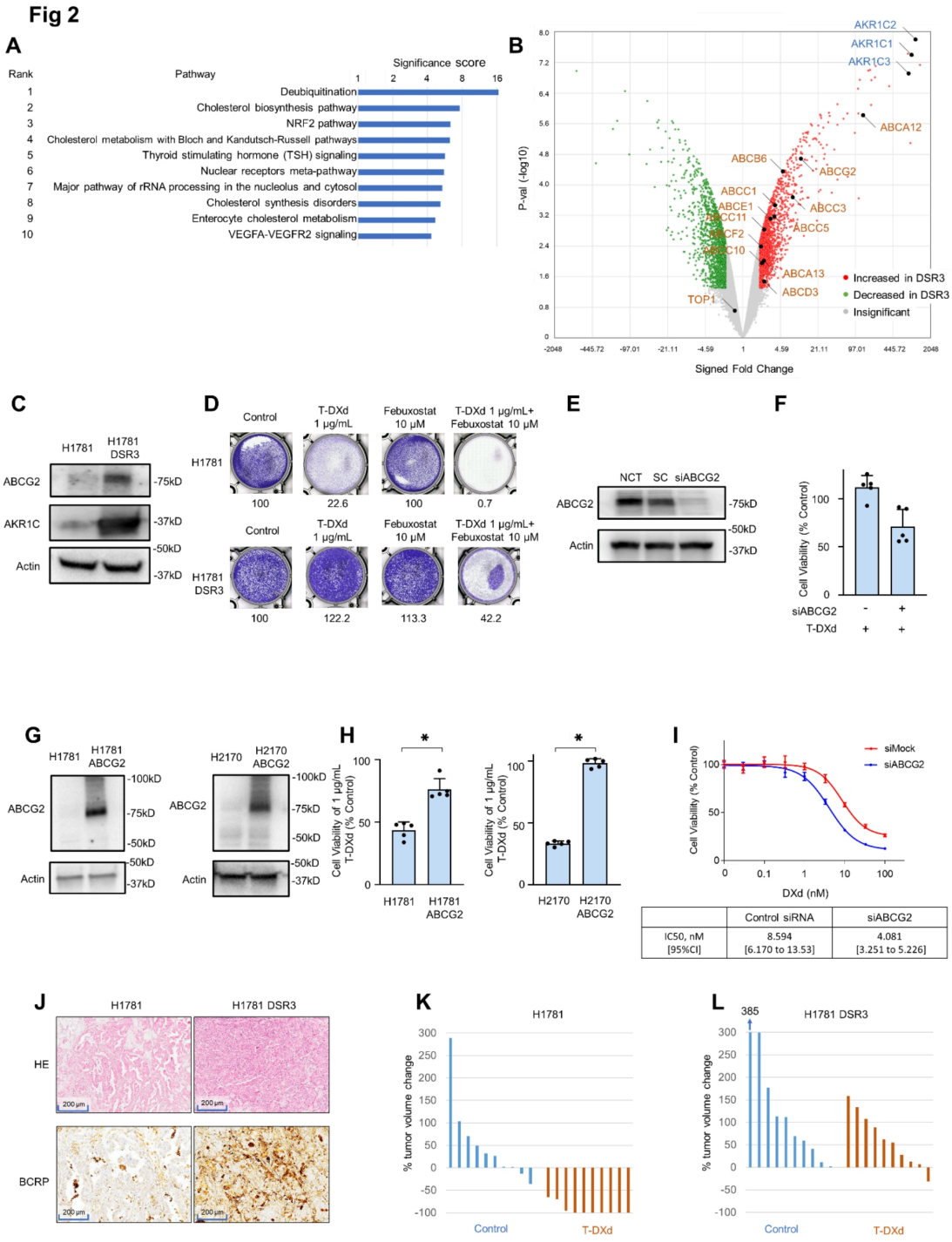


Figure 2

Upregulated ABCG2 in H1781DSR3 cells and its involvement in T-DXd resistance.

(A) Pathway analysis of differentially expressed transcripts between H1781DSR3 and parental H1781 cells using Transcriptome Analysis Console v4.0.3, ranked by significance score.

(B) Volcano plot of microarray data from two biological replicates per cell line. Each point represents a transcript; axes indicate signed fold change and −log10(P value), calculated using ANOVA. Red, green, and gray indicate upregulated, downregulated, and nonsignificant transcripts, respectively (absolute fold change ≥ 2; $P < 0.05$).

(C) Western blot analysis of AKR1C and ABCG2 in H1781 and H1781DSR3 cells.

(D) High-density growth assays following treatment with T-DXd (1 μg/mL), febuxostat (10 μM), or both for 14 days. Crystal violet-stained areas were quantified using ImageJ and normalized to untreated controls. Representative images from two independent experiments are shown.

(E) Western blot analysis of ABCG2 in H1781DSR3 cells 72 h after transfection with negative control (NC), scrambled, or ABCG2-targeting siRNA.

(F) Viability of H1781DSR3 cells transfected with NC or ABCG2-targeting siRNA and treated with T-DXd (10 μg/mL) for 5 days, normalized to untreated controls. Mean ± SD (n = 5 independent experiments); unpaired t-test, $P < 0.05$.

(G) Western blot analysis of ABCG2 in parental H1781 and H2170 cells and their ABCG2-overexpressing derivatives.

(H) Viability of parental and ABCG2-overexpressing H1781 and H2170 cells treated with T-DXd (1 μg/mL) for 5 days, normalized to untreated controls. Mean ± SD (n = 5 independent experiments); unpaired t-test, *$P < 0.05$.

(I) DXd dose–response curves in H1781DSR3 cells transfected with NC or ABCG2-targeting siRNA and treated for 72 h. Viability was normalized to untreated controls. Mean ± SEM (n = 6 replicates). IC50 values and 95% confidence intervals were estimated by nonlinear regression.

(J) Representative HE and BCRP immunohistochemical staining of H1781 and H1781DSR3 xenografts.

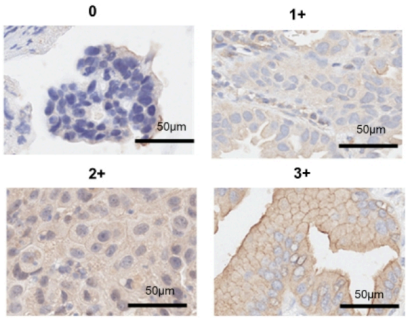
(K, L) Waterfall plots of tumor-volume changes in H1781 (K) and H1781DSR3 (L) xenografts at day 21 relative to day 1. T-DXd (3 mg/kg) was administered intraperitoneally once on day 1. Each bar represents one mouse (n = 10/group).

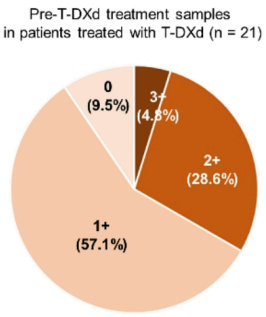
ABCG2, ATP-binding cassette subfamily G member 2; AKR1C, aldo-keto reductase family 1 member C; T-DXd, trastuzumab deruxtecan; DXd, deruxtecan; NC, negative control; SD, standard deviation; BCRP, breast cancer resistance protein; ANOVA, analysis of variance; IHC, immunohistochemistry; CI, confidence interval; SEM, standard error of the mean; IC50, half-maximal inhibitory concentration.

Fig 3

A

Patient No.	Sex	Age	Mutation type	Best overall response	PFS (months)	Ongoing T-DXd treatment at data cutoff	BCRP score, Pre	BCRP score, Post
1	Female	48	G770_A771ins	SD	11.7	No	**2+**	**3+**
2	Female	50	G776delinsVC	PR	10.7	No	**1+**	**3+**
3	Male	68	E770_A771ins	PR	9.1	No	**1+**	**3+**
4	Male	56	G770_A771ins	SD	9.3	No	**1+**	**3+**
5	Male	78	A775-G776insYVMA	PR	6.5	No	**1+**	**3+**
6	Male	68	A775-G776insYVMA	SD	8.6	Yes	**2+**	N.D
7	Female	41	A775-G776insYVMA	PR	6.2	No	**1+**	N.D
8	Female	33	G770_A771insAYVM	PR	16.5	Yes	**1+**	N.D
9	Female	69	G770_A771insAYVM	SD	11.1	No	**1+**	N.D
10	Female	77	G770_A771insAYVM	PD	1.4	No	**3+**	N.D
11	Female	42	G776delinsVC	SD	4.4	No	**2+**	N.D
12	Male	69	G770_A771ins	PR	17.5	Yes	**1+**	N.D
13	Male	71	A771-Y772insYVMA	PD	1.5	No	**2+**	N.D
14	Female	82	A775_G776insYVMA	Not administered	-	-	**1+**	N.D
15	Female	53	G778_P780insGSP	SD	3.2	No	**2+**	N.D
16	Male	61	A775-G776insYVMA	PR	3.7	No	**0**	N.D
17	Male	76	A775-G776insYVMA	Not administered	-	-	**2+**	N.D
18	Male	79	V777L	Not administered	-	-	**1+**	N.D
19	Male	70	A775-G776insYVMA	Not administered	-	-	**2+**	N.D
20	Male	59	A775_G776insYVMA	PR	6.9	Yes	**0**	N.D
21	Male	64	A775_G776insYVMA	PR	14.0	No	**1+**	ND
22	Male	80	G776delinsVC	PR	13.4	No	**1+**	**1+**
23	Male	76	A775_G776insYVMA	PR	8.4	No	**1+**	ND
24	Male	64	A775_G776insYVMA	PD	1.4	No	**2+**	ND
25	Male	61	A775_G776insYVMA	PR	4.4	No	**1+**	ND





D

Best overall response	Low BCRP (n=14)	High BCRP (n=7)
PR	12	0
SD	2	4
PD	0	3
ORR	85.7%	0%

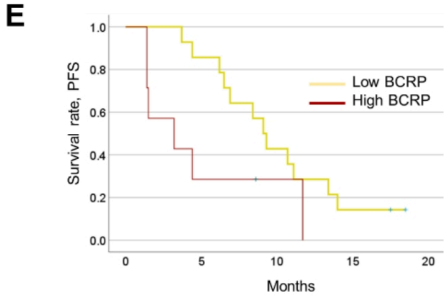


Figure 3

BCRP expression in HER2-mutant NSCLC tumors before and after T-DXd treatment and its association with clinical outcomes.

(A) Clinical characteristics of patients with HER2-mutant NSCLC who received T-DXd (n = 21) and those who did not (n = 4).

(B) Representative images of BCRP immunohistochemical staining in NSCLC tumor tissues. BCRP expression was scored as 0, 1+, 2+, or 3+ based on membranous staining patterns, as described in Methods.

(C) Distribution of pretreatment BCRP IHC scores in patients treated with T-DXd (n = 21).

(D) Best overall response to T-DXd according to pretreatment BCRP expression (n = 21). Low BCRP was defined as IHC scores 0 or 1+, and High BCRP as 2+ or 3+. Response rates were compared using a two-sided Fisher's exact test.

(E) Kaplan–Meier curves for progression-free survival (PFS) following T-DXd treatment according to pretreatment BCRP expression.

(F) HE staining and BCRP immunostaining of paired tumor specimens obtained before T-DXd treatment and after disease progression in six patients.

(G) Comparison of paired BCRP IHC scores before treatment and after disease progression (n = 6). Statistical significance was assessed using the Wilcoxon matched-pairs signed-rank test (p = 0.0625).

ABCG2, ATP-binding cassette transporter G2; BCRP, breast cancer resistance protein; HE, hematoxylin and eosin; IHC, immunohistochemistry; NSCLC, non-small cell lung cancer; PFS, progression-free survival; PR, partial response; SD, stable disease; PD, progressive disease; ORR, overall response rate; ND, not done; T-DXd, trastuzumab deruxtecan.

Fig 4

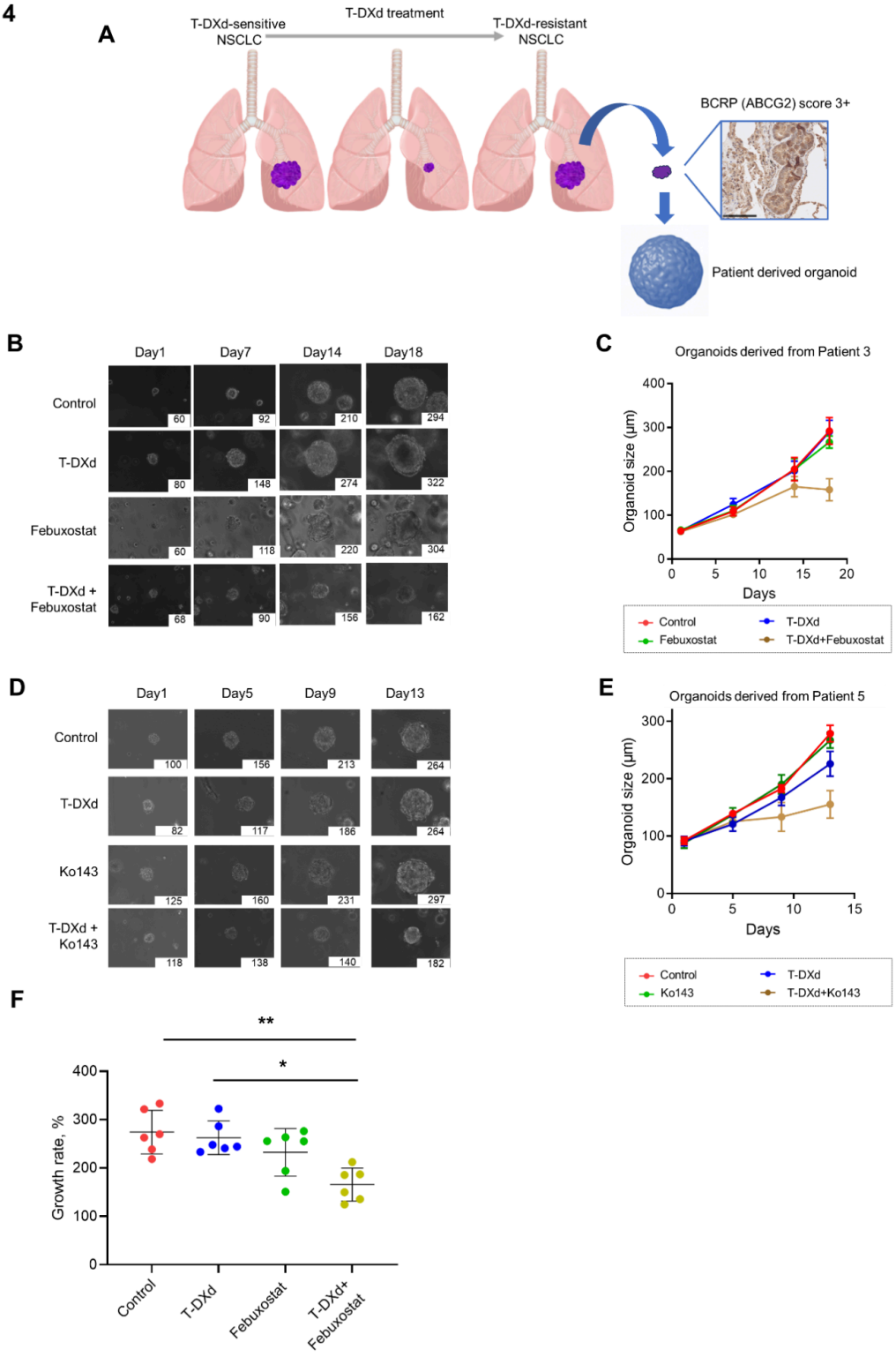


Figure 4

ABCG2 inhibition restores T-DXd sensitivity in patient-derived HER2-mutant NSCLC organoids.

(A) Schematic workflow for establishing patient-derived tumor organoids.

(B, D) Representative bright-field images of tumor organoids derived from patients 3 (B) and 5 (D). Organoids were treated with T-DXd (1 μg/mL), febuxostat (10 μM; B) or Ko143 (10 μM; D), or their respective combinations for 18 days (B) or 13 days (D). Numbers below the images indicate organoid diameters (μm).

(C, E) Longitudinal changes in organoid diameters corresponding to panels B and D, respectively. Six organoids per treatment group were cultured in a single well and monitored over time. Data are presented as mean ± SEM. No inferential statistical comparisons were performed because organoids within each group shared the same well.

(F) Relative growth of organoids derived from patient 5 following treatment with T-DXd (1 μg/mL), febuxostat (10 μM), or their combination for 13 days. One organoid was cultured per independent well (n = 6 wells per group). Relative growth (%) was calculated as (diameter on day 13 / diameter on day 1) × 100. Data are presented as mean ± SD. Statistical significance was assessed using one-way ANOVA followed by Tukey's multiple comparisons test. *P = 0.0032, **P = 0.0011.

T-DXd, trastuzumab deruxtecan; HER2, human epidermal growth factor receptor 2; NSCLC, non-small cell lung cancer; SEM, standard error of the mean; ANOVA, analysis of variance.

Fig 5

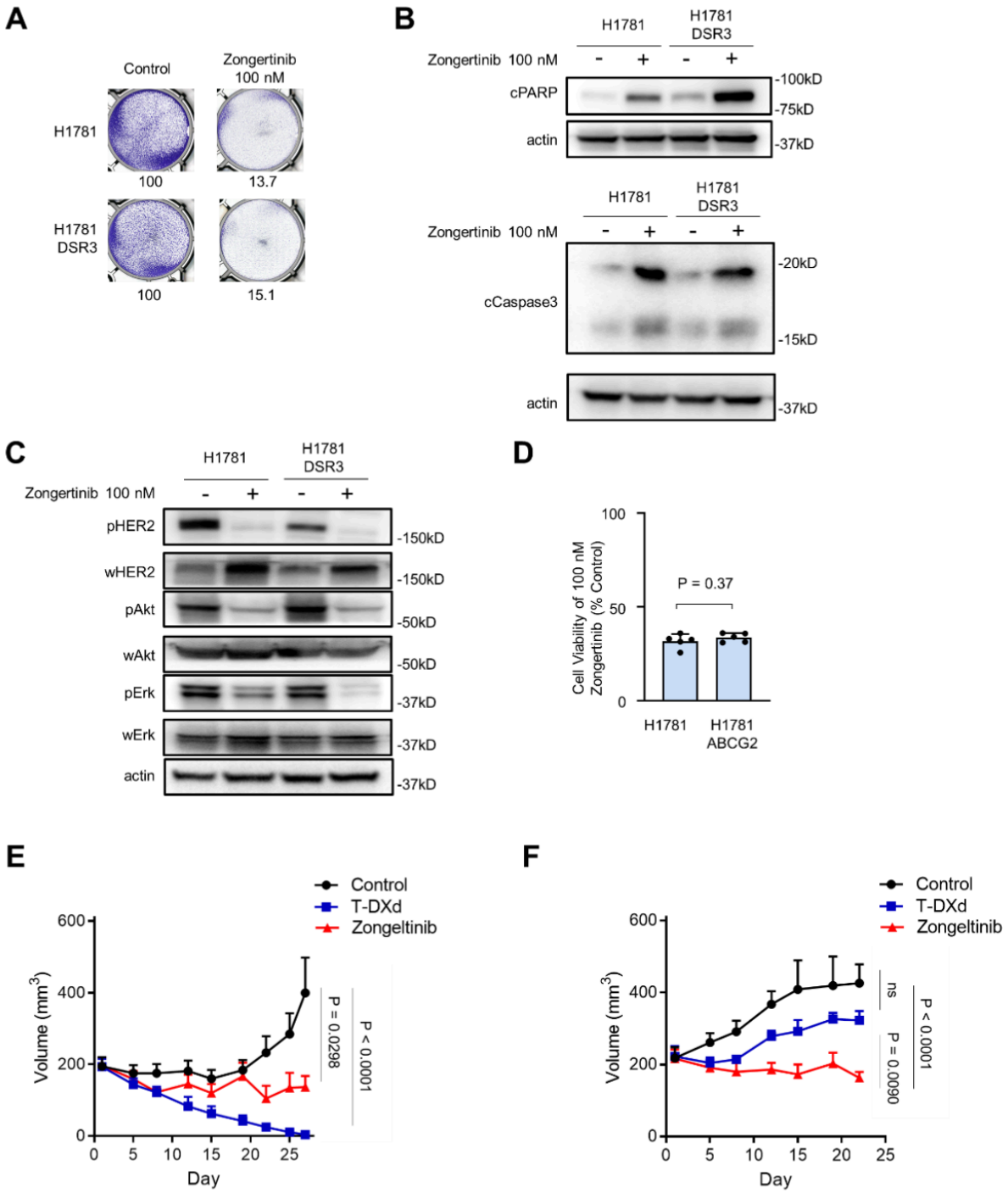


Figure 5

Zongertinib retains antitumor activity in T-DXd-resistant H1781DSR3 cells.

(A) High-density growth assays of parental H1781 and T-DXd-resistant H1781DSR3 cells treated with or without 100 nM zongertinib were analyzed by western blotting.

(D) Cell viability of H1781 and ABCG2-overexpressing H1781ABCG2 cells following treatment with or without 100 nM zongertinib for 5 days. Cell viability was normalized to that of the corresponding untreated controls and expressed as a percentage. Statistical comparisons were performed using an unpaired t-test. Mean ± SD (n = 6 independent experiment)

(E, F) Antitumor efficacy of T-DXd and zongertinib in mouse xenograft models established from parental H1781 (E) and T-DXd-resistant H1781DSR3 (F) cells. Mice received T-DXd (3 mg/kg, single intraperitoneal injection on day 1), zongertinib (10 mg/kg, orally once daily on weekdays from day 1 until the final tumor measurement), or vehicle control (n = 10 mice per group). Tumor volumes are presented as mean ± SEM. Tumor volumes at the final measurement were compared using one-way ANOVA followed by Tukey's multiple-comparisons test. Exact P values are indicated in the graphs.

T-DXd, trastuzumab deruxtecan; HER2, human epidermal growth factor receptor 2; ANOVA, analysis of variance; SEM, standard error of the mean; ns, not significant.

for 14 days. Crystal violet-stained areas were quantified using ImageJ. Representative images from two independent experiments are shown.

(B, C) H1781 and H1781DSR3 cells were treated with or without 100 nM zongertinib for 72 h. Apoptosis-related proteins (B) and HER2 downstream signaling proteins (C)

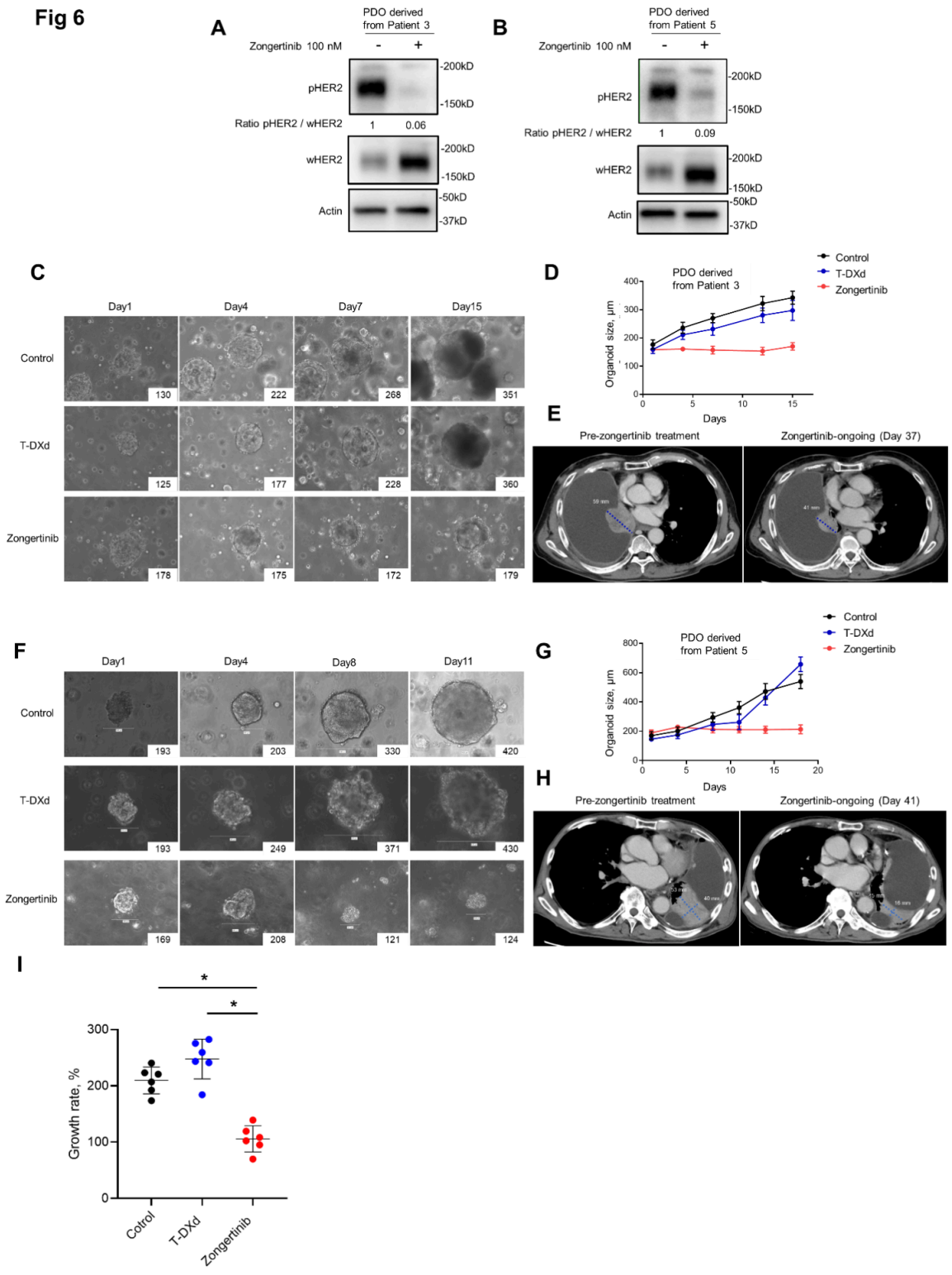


Figure 6

Zongertinib exhibits antitumor activity in T-DXd-resistant patient-derived organoid models.

(A, B) Patient-derived organoids (PDOs) from patients 3 (A) and 5 (B) were treated with 100 nM zongertinib for 3 days. HER2 phosphorylation and protein expression were assessed by western blotting. Phosphorylated HER2 band intensities were normalized to total HER2.

(C, D) Representative bright-field images of patient 3-derived organoids treated with vehicle, T-DXd (1 μg/mL), or zongertinib (100 nM) for 15 days (C). Numbers indicate organoid diameters (μm). Diameters of six organoids cultured in a single well per treatment group were monitored longitudinally (D).

(E) Contrast-enhanced computed tomography (CT) images of patient 3 before and during zongertinib treatment.

(F, G) Representative bright-field images of patient 5-derived organoids treated with vehicle, 1 μg/mL T-DXd, or 100 nM zongertinib for 18 days (F). Numbers indicate organoid diameters (μm). Diameters of six organoids cultured in a single well per treatment group were monitored longitudinally (G).

(H) Contrast-enhanced CT images of patient 5 before and during zongertinib treatment.

(I) Relative growth of patient 5-derived organoids treated with vehicle, 1 μg/mL T-DXd, or 100 nM zongertinib for 13 days. Six independent wells per group contained one organoid each (n = 6). Relative growth (%) was calculated as (diameter on day 13/diameter on day 1) × 100. Statistical comparisons were performed using one-way ANOVA followed by Tukey's multiple comparisons test.

Data in (D), (G), and (I) are presented as mean ± SEM. No inferential statistical comparisons were performed for (D) and (G) because organoids within each treatment group shared a single well.

T-DXd, trastuzumab deruxtecan; HER2, human epidermal growth factor receptor 2; SEM, standard error of the mean; ANOVA, analysis of variance.

Supplementary Files

This is a list of supplementary files associated with this preprint. Click to download.

- Supplementarymaterials.2026.10.26.pdf
- SupprementaryData.2026.10.26.xlsx